

## Preliminary analysis of Lower Cretaceous metadolerites drilled in Lower Austria – a tribute to Prof. Csaba SZABÓ

TARI, Gábor<sup>1</sup>, VRŠIČ, Aleš<sup>2</sup>, HUJER, Wolfgang<sup>2</sup>, MEKONNEN, Elias<sup>2</sup>, SCHNEIDER, David A.<sup>3</sup>, PÉCSKAY, Zoltán<sup>4</sup>, SZEPESI, János<sup>4,5</sup>

<sup>1</sup>OMV Upstream, Vienna, Austria, gabor.tari@omv.com

<sup>2</sup>OMV Upstream, TECH Center & Laboratory, Gänserndorf, Austria

<sup>3</sup>University of Ottawa, Canada

<sup>4</sup>HUN-REN Institute for Nuclear Research, Geochronology Group, Debrecen, Hungary

<sup>5</sup>HUN-REN-ELTE, Volcanology Research Group, Budapest, Hungary

### *Alsó-Ausztriában fúrt, alsó kréta bazalt teleptelések előzetes vizsgálata – tisztelgés SZABÓ Csaba professzor munkássága előtt*

#### Összefoglalás

Két kutatófúrás révén az 1960-as évek eleje óta ismert számos teleptelér előfordulása a Molasse-medencében (Ausztria északkeleti részén). A feltételezett dogger (Porrau-2) és felső paleozoikum (Roggendorf-1) üledékes rétegsorban megjelenő, erősen átalakult metadoleritek a korábbi értelmezések szerint is intruzív jellegűek, a telérek kora, valamint azok tágabb rétegtani és tektonikai vonatkozásai azonban nem kellően tisztázottak.

Mintegy 60 év elteltével, ebben a munkában különböző modern analitikai módszerek alkalmazásával az intruzívumok új értelmezését javasoljuk. Eredetileg a metadoleritek korát jura korúnak tekintették. Új, de még előzetes eredményeink azonban kora kréta korú (136–141 Ma) intruzív vulkanizmust jeleznek, amelyre nemcsak a K-Ar kormeghatározás eredménye utal, hanem a teleptelések regionális analógiái is. A Porrau-2 fúrás alsó, feltételezett dogger szekvenciájából származó egyetlen dácitmintát egy régebbi intruzív elemként értelmeztünk, mivel a K-Ar kormeghatározás (283–284 Ma) alsó perm korra utal. Tehát a kút mélyebb részén feltárt rétegek nem lehetnek dogger korúak, hanem a felső paleozoikumba tartoznak (perm). Ezért a Porrau-2 és Roggendorf-1 kutakban található alluviális-fluviális üledékek egy része a csehországi Morávia karbon–perm Boskovice-medencének a felszín alatti, délnyugati folytatását képviseli Alsó-Ausztriában.

Regionális léptékben a vizsgált magmás kőzetek petrográfiája hasonlónak tűnik a jól ismert alsó kréta alkáli vulkáni kőzetekkel (lamprofir, bazanit, fonolit), amelyek a morva-sziléziai Beszkidek területén, az Északkelet-Csehországban és Dél-Lengyelországban, valamint a dél-magyarországi Mecseki Zónában fordulnak elő. Míg mindezek a vulkáni egységek jelenleg az eredeti paleogeográfiai helyzetükből elmozdult, alpesi allochthon övekben helyezkednek el, addig a tanulmányunkban szereplő alsó kréta teleptelések az autochton európai lemezben találhatóak. Ezért fontos, új támpontot nyújtanak a kora kréta kori, regionális rift zóna palinspasztikus rekonstrukciójához a mezozoikum európai lemez déli peremén.

*Tárgyszavak: diabáz(bazalt), teleptelér, kora kréta, Ausztria, Magyarország, Tisza mega-egység, riftesedés*

#### Abstract

The occurrences of numerous sills penetrated in two exploration wells drilled in the Molasse Basin in NE Austria were known since the early 1960s. Although the initial analysis of these strongly altered metadolerite units intercepted in an apparently Dogger (Porrau-2) and Upper Paleozoic (Roggendorf-1) clastic sequence correctly concluded about their intrusive character, the age relationships and the broader stratigraphic and tectonic implications remained poorly constrained.

After about 60 years, using various modern analytical methods, a new understanding of these intrusives is outlined in this contribution. Originally, the age of the metadolerites was considered as Jurassic. However, our new, preliminary results provided an Early Cretaceous age (136–141 Ma) for the intrusive volcanism not only indicated by K-Ar age determination but also by regional analogues for the sills. A single dacite sill from the lower, supposedly Dogger sequence of the Porrau-2 well is interpreted as an older intrusive unit and its K-Ar date (283–284 Ma) suggests an Early Permian age. Hence the sequence drilled in the deeper part of this well cannot be Dogger in age but instead it is Upper Paleozoic (Permian). Therefore, some of the alluvial-fluvial clastics in the Porrau-2 and Roggendorf-1 wells represent the subsurface southwestern continuation of the Carboniferous–Permian Boskovice Trough from Moravia into Lower Austria.

On a regional scale, the petrography of the studied sills appears to be similar to the well-studied Lower Cretaceous alkaline igneous rocks (lamprophyres, basanites, phonolites) occurring in the Moravian-Silesian Beskidy area in north-east Czech Republic and southern Poland and in the Mecsek Zone of southern Hungary. Although all these volcanic units are presently located in Alpine thrust-fold belts displaced from their original paleogeographic position, the sills in our study are anchored within the autochthonous European plate. Therefore, they provide an important new constraint for the palinspastic reconstruction of the regional-scale Early Cretaceous rift zone along the southern margin of the Mesozoic European plate.

*Keywords: diabase/basalt, sill, Early Cretaceous, Austria, Hungary, Tisza Mega-unit, rifting*

## Introduction

Among the many wells drilled in the foreland region of the Eastern Alps in Austria (Figure 1), there are only two which penetrated unusual and highly altered volcanics with a basaltic composition. These diabase (former name of the altered basaltic sills) units were found within Dogger and upper Paleozoic sedimentary units in the Porrau-2 and Roggendorf-1 wells (Figures 2 & 3), respectively (WIESENER

1965, WIESENER et al. 1976, WESSELY 2006, ROETZEL et al. 2009). These magmatic rocks were described as Jurassic sills which intruded into the Mesozoic-Paleozoic cover sequence above the crystalline basement of the Bohemian Massif. An apparent difficulty of the age assignment stems from the fact that lithologically, the coarse-grained clastics of the Middle Jurassic and the Permian–Carboniferous sequences are very similar. Besides the poorly constrained age relationships between the sills and the host rocks, the struc-

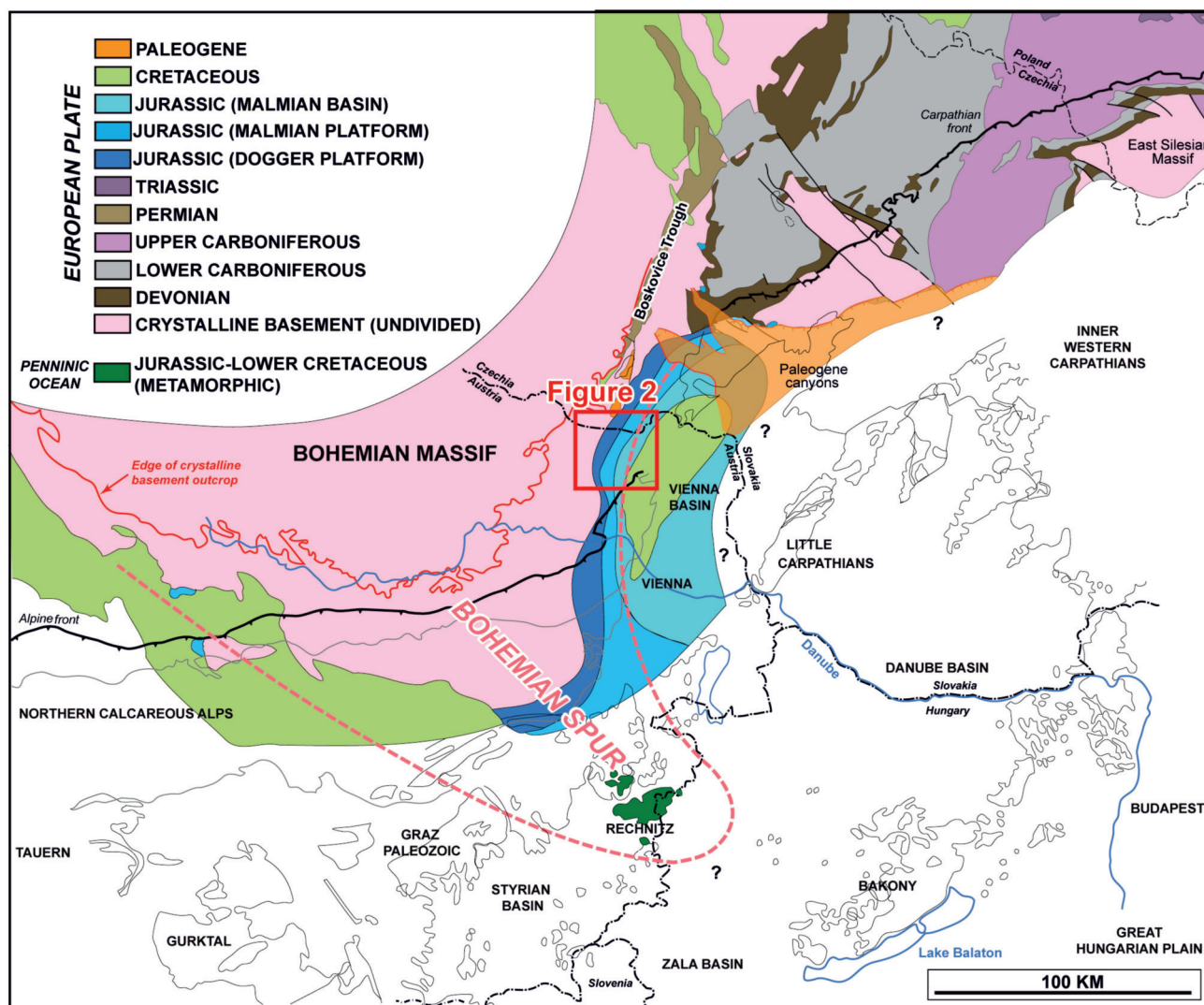


Figure 1. Location of the study area in NE Austria in the framework of the autochthonous cover and basement of the European margin (modified from TARI 2005)  
 1. ábra. A vizsgált terület elhelyezkedése Északkelet-Ausztriában az európai perem autochton fedőjének és aljátának a kontextusában (TARI 2005) alapján

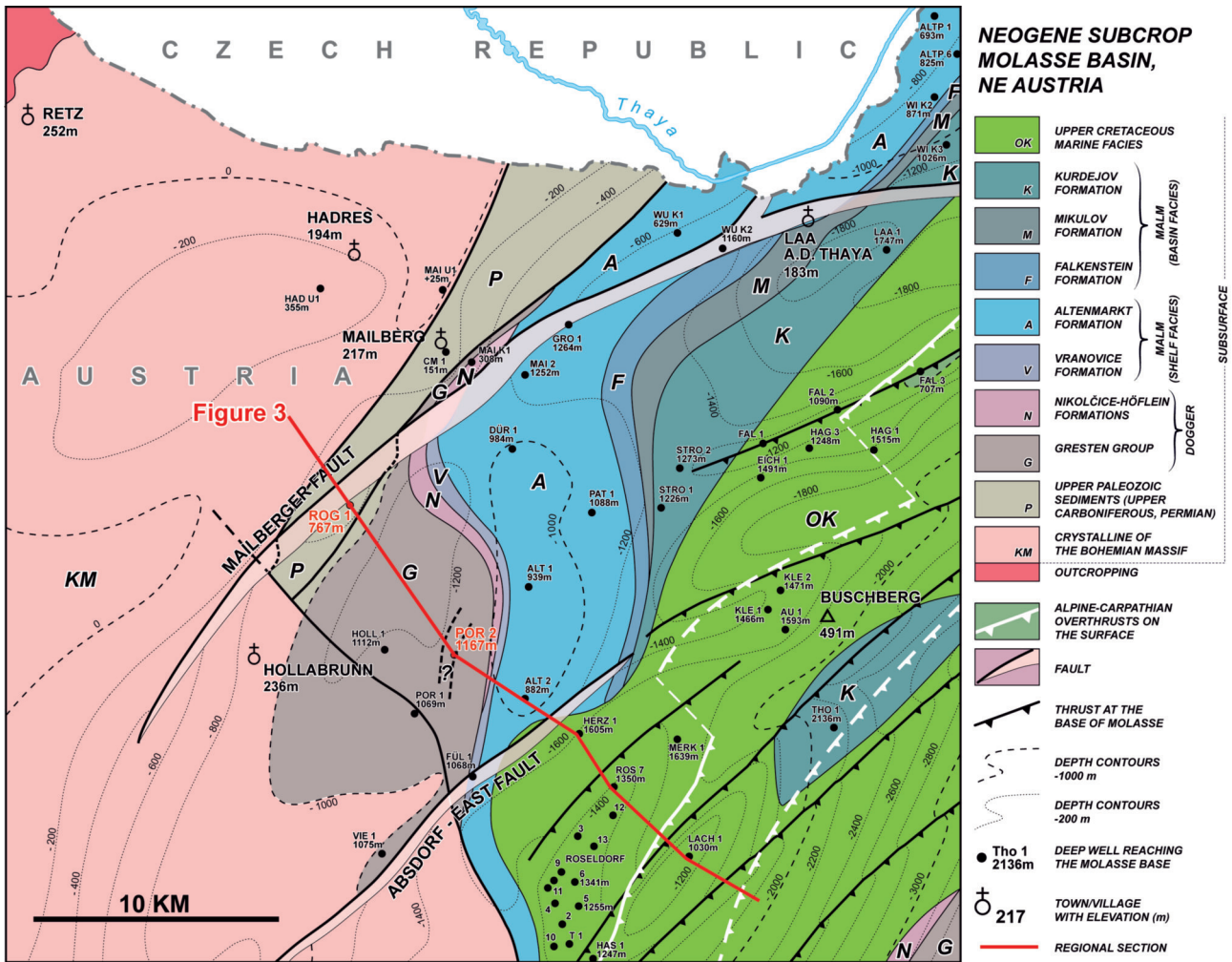


Figure 2. Sub-regional setting of the Porrau-2 and Roggendorf-1 wells drilled in Lower Austria in the eastern Molasse Basin  
 2. ábra. A Porrau-2 és Roggendorf-1 fúrások szubregionális elhelyezkedése Alsó-Ausztriában, a keleti Molassz-medencében

tural context of the Porrau-2 well was left open-ended due to the lack of seismic reflection data across this well. Existing illustrations of the Porrau-2 depict either a fault-related near-vertical metadolerite body (ROETZEL et al. 2009; Figure 3) or a steep folded feature (Figure 4) with dips meant to explain the near-vertical Dogger sedimentary layers observed in the cores of the well (WESSELY 2006). The main aim of this contribution is to document new data on both the intrusives and the sediments of the Porrau-2 well. These data clarified some of the ambiguous aspects of the existing interpretations in a preliminary fashion and highlighted the need for more analytical work to firm up the interpretations in this paper.

The results of the present study also provided a new, large-scale perspective on the Lower Cretaceous intrusives penetrated in the Porrau-2 and Roggendorf-1 wells. Contemporaneous volcanic-magmatic rocks (Berriasian to Valanginian) with broadly similar lithological characteristics are known in the External Carpathians (Silesian Beskid Mts.) and the Western Carpathians of Poland and Slovakia, (SPIŠIAK 2002, HARANGI et al. 2003, SPIŠIAK et al. 2011, SZOPA et al. 2014, MADZIN et al. 2014, CSIBRI et al. 2020). Lower Cre-

taceous volcanics were also documented in the Ukrainian Outer Carpathians, close to the Polish border (HNYLKO et al. 2015, KROBICKI et al. 2015).

On an even larger scale, the Early Cretaceous alkaline basalt magmatism is one of the most characteristic features of the Mecsek Unit in southern Hungary (HARANGI & ÁRVA-SOÓS 1993; HARANGI 1994; HARANGI et al. 1996, 2003). Products of this rifting-related magmatism outcrop in the Mecsek Mts. and can also be traced in the subsurface in other parts of southern Hungary beneath the Pannonian Basin (HAAS & PÉRO 2004). The main phase of the volcanism in southern Hungary occurred during the Early Cretaceous, mainly in the Valanginian, although it extended into the Hauterivian (Mecsekjános Basalt Complex). In the western Mecsek Mts. basaltic and trachytic small intrusions and dikes are typical, whereas in the eastern part rocks of basalt-tephrite-phonolite series and alkali-trachyte occur in various proportions (KUBOVICS et al. 1990). The presence of pillow lavas, lava breccias, and hyaloclastites indicate submarine volcanism. Dikes, sills, and subvolcanic bodies are also common. The geochemical, mineralogical and petrographic features of the Mecsek volcanic-magmatic rocks suggest



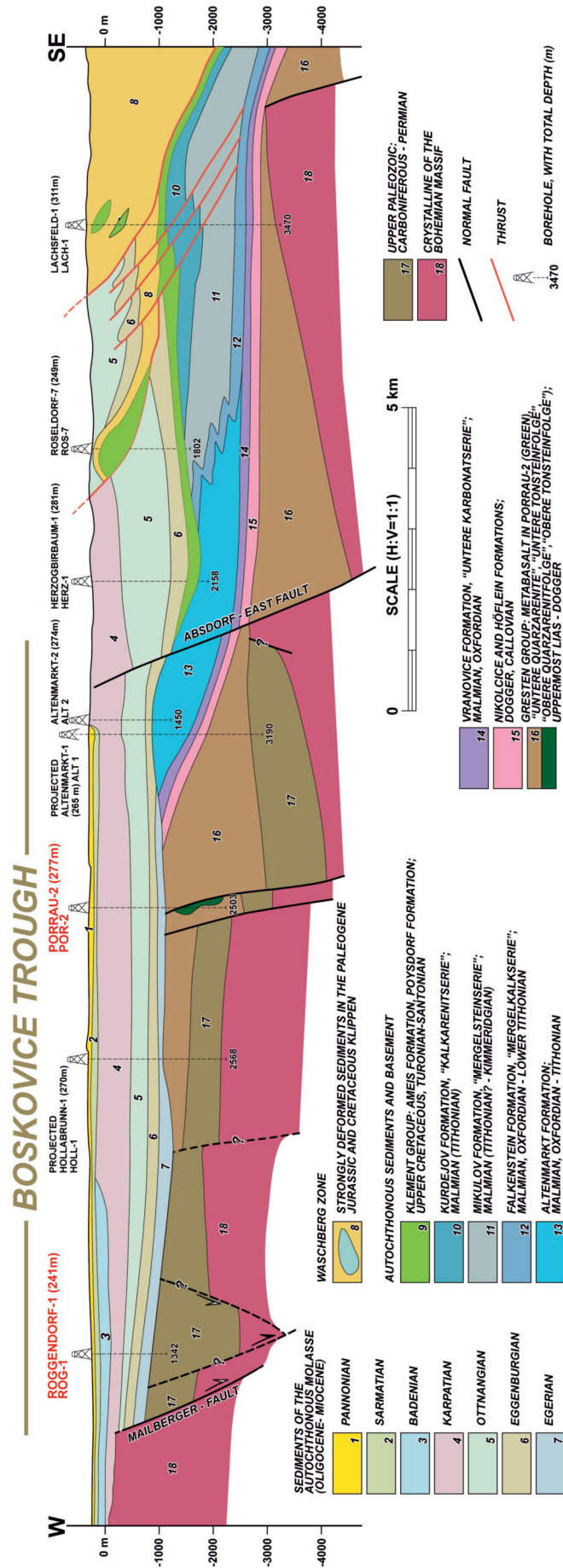


Figure 3. Cross-section showing the position of the Porrau-2 and Roggendorf-1 wells in the foreland of the eastern end of the Eastern Alps (modified from ROETZEL et al. 2009). No vertical exaggeration

3. ábra. A Porrau-2 és a Roggendorf-1 fúrások helyzetét bemutató keresztmetszvény a Keleti-Alpok Keleti végének az előterében (Roetzcel et al. 2009 adatai alapján). Nincs függőleges túlmagyasítás



continental rift-type volcanism (KUBOVICS & BILLIK 1984, HARANGI et al. 1996).

The secondary aim of this work is to highlight the importance of the autochthonous nature of the Lower Cretaceous metadolerites of Lower Austria emplaced within the European margin. They provide an important new map-view constraint for the palinspastic reconstruction of the large Early Cretaceous rift zone along the southern margin of the Mesozoic European plate. Large mega-units, such as the Tisza and West Carpathians were separated from Europe along this rift zone.

### Regional setting of the studied wells in NE Austria

The crystalline basement of the Molasse zone in Eastern Austria (Figure 1) is covered by Mesozoic and Paleozoic sediments (WESSELY 2006). Within Dogger clastic sediments, the Porrau-2 well, drilled in 1960/61 to a final depth of 2503.0 m by OMV, penetrated numerous layers of diabases (Figures 1, 4 & 5) classified and described by WIESENEDER (1965). His work was focused on the sequence drilled between 1700–2000 m depth where at least 11 metadolerite units were documented in cores. It was suggested that the strongly altered metadolerites (or diabases) in the well were intruded as sills during the Jurassic (WIESENEDER 1965).

Based on the core description of the deeper part of the borehole no more metadolerite was found below 2000 m, however, there are conglomerates with volcanic clasts embedded in them. The apparent reworking of the volcanic

material into the sedimentary units in between contradicts the intrusive character of the metadolerites but instead would imply the presence of extrusive units, such as lavas. Also, a tuffite layer was reported by WIESENEDER (1965) at about 1814 m depth which we could not locate in the core material. Instead, our work indicated potential tuffs at about 1895-1897 and at 1960 m. The presence of tuff and tuffite also implies extrusive volcanic activity.

In a second drill hole, Roggendorf-1, drilled in 1962 to a final depth of 1342.0 m by OMV, sedimentary rocks of Paleozoic age were found below about 1000 m (Figure 5). These siliciclastic rocks contain intercalations of quartz porphyrites, metadiabases, igneous breccias, rhyolitic tuffites and tuffs (WIESENEDER et al. 1976). Upper Paleozoic (Carboniferous, Permian) sediments described in the subsurface of the region are typically grey, partly greenish quartz arenites alternating not only with dark, partly reddish violet claystones, but also with quartz/feldspar breccias. In the Upper Carboniferous sediments, coal seams often occur (BRIX & GÖTZINGER 1964, BRIX 1993). However, coal seams have been also reported from the Permian succession.

Structurally, two very large fault zones define the syn-rift architecture of the study area (Figure 3), the Mailberger and the Absdorf-East faults (KRÖLL & WESSELY 2001). Along the Mailberger fault, the normal offset is as large as 700 m. The fault was still active during the Cenozoic, but its main activity was during the Dogger (WESSELY 2006) and quite possibly even during the Permian with large syn-sedimentary displacement. Similarly, the Absdorf-East Fault is a reactivated syn-rift fault which has a considerable offset especially within the Dogger sequence (Figure 3). Syn-rift

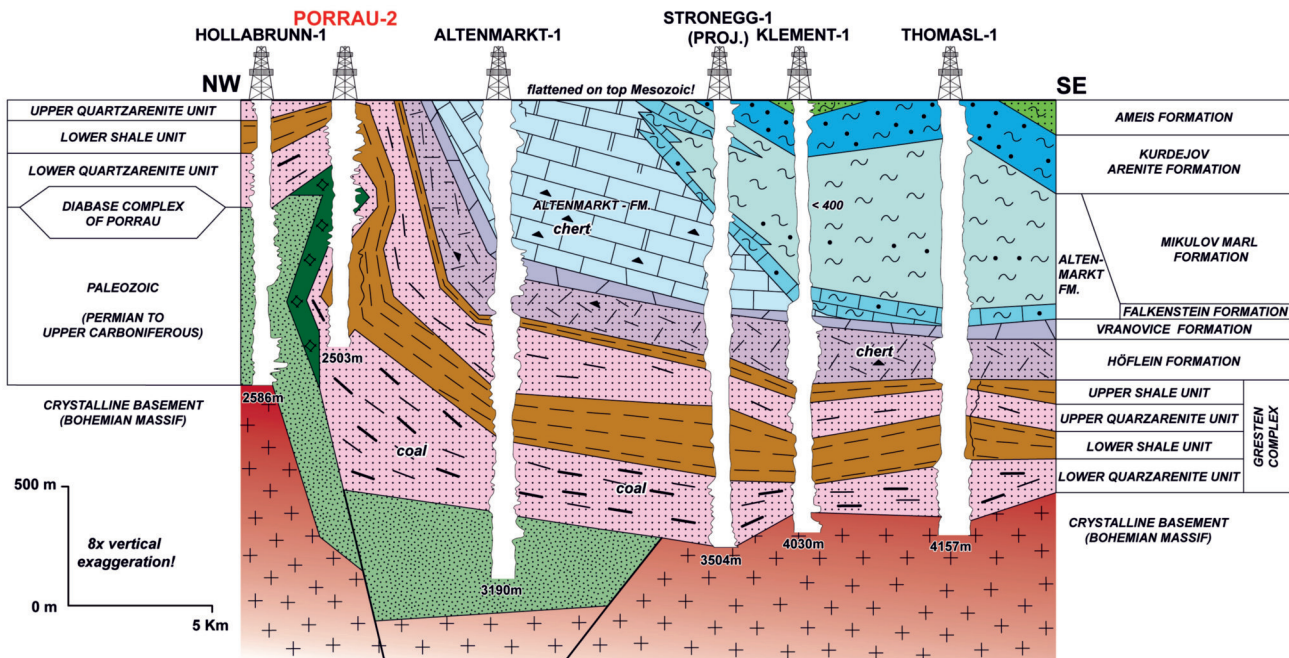
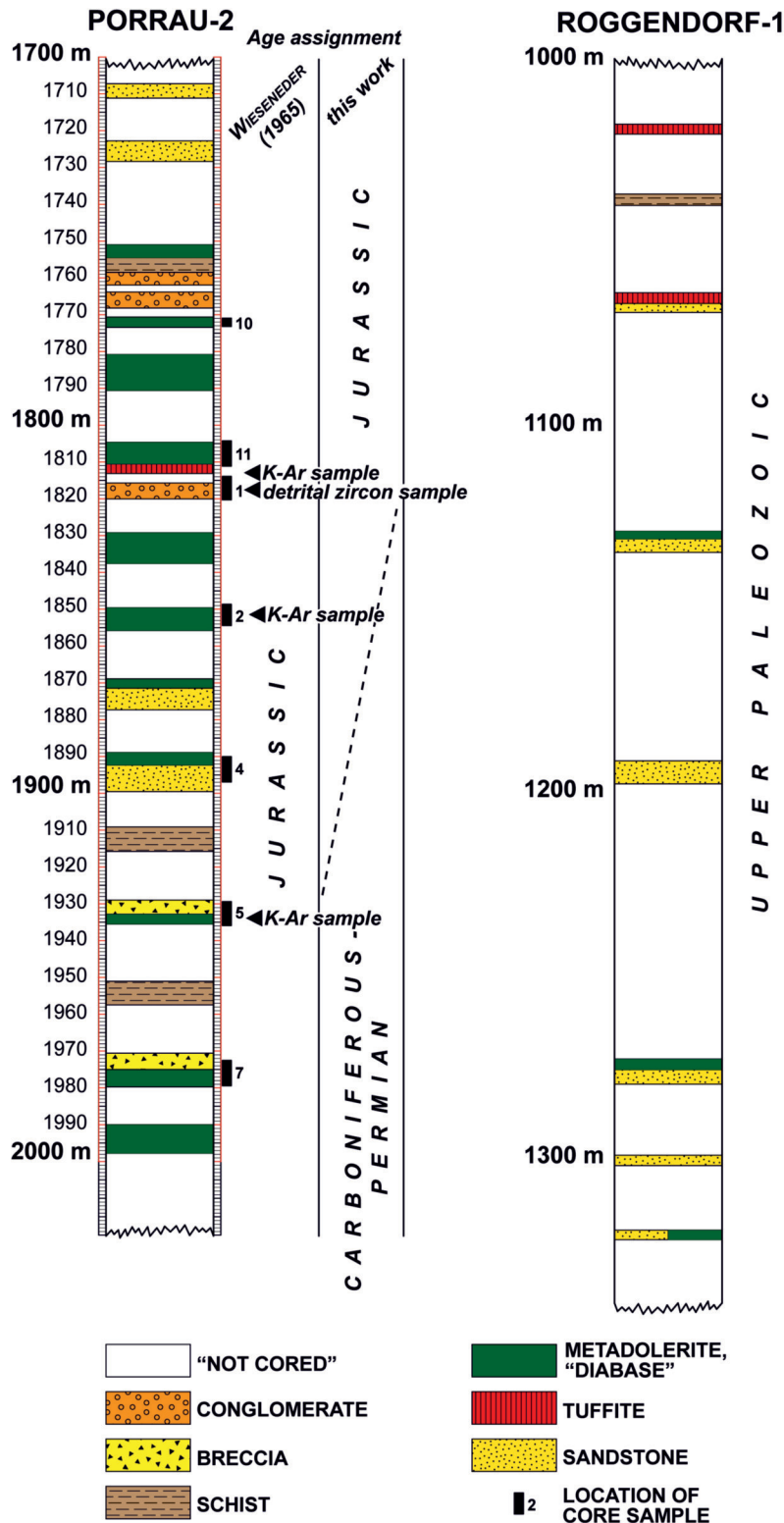


Figure 4. Sub-regional scale section across the Porrau-2 well (redrawn from WESSELY 2006). Note that the section is flattened on top of the Mesozoic sequence. Vertical exaggeration is 8x

4. ábra. A Porrau-2 kút szubregionális léptékű szelvénye (WESSELY 2006) alapján). Megjegyzendő, hogy a szelvény a mezozoikus szekvencia tetején van kiegyenlítve. A függőleges túlmagyasítás 8x



**Figure 5.** Simplified lithologic columns of the a) Porrau-2 and b) Roggendorf-1 wells in their deeper segments where subvolcanic rocks (shown in dark green) were penetrated (modified from WIESENEDER 1965). Location of the samples for thin section characterization, K-Ar dating, and detrital zircon dating are also shown. Note that based on our new results, there is an alternative age assignment for a large part of the section in the Porrau-2 well

5. ábra. Az a) Porrau-2 és b) Roggendorf-1 fúrások egyszerűsített litológiai oszlopai a mélyebb szakaszaikban, ahol szubvulkáni kőzeteket (sötétzöld színnel jelölve) fúrtak (WIESENEDER 1965 alapján módosítva). A vékonycsiszolatos jellemzéshez, K-Ar kormeghatározáshoz és detritális cirkon kormeghatározáshoz használt minták elhelyezkedése is látható. Megjegyzendő, hogy az új eredményeink alapján a Porrau-2 fúrás esetében új geokronológiai értelmezéseket közlünk

faulting is responsible for the formation of all the asymmetrical half-grabens in the broader area, such as those east of Mailberg, east of Hagenberg and of Stockerau (Figure 2).

Another fault zone, striking perpendicular to the above mentioned major syn-rift master faults must be responsible for the termination of the Paleozoic and Mesozoic units towards the southwest near Hollabrunn (Figure 2). This transpressive cross-faulting was assumed to cause the steepness of the Dogger sequence (Figures 3, 4), with the metadolerite embedded in it, in the case of the Porrau-2 borehole (WESSELY 2006, ROETZEL et al. 2009).

The sub-regional scale section across the Porrau-2 and some other wells illustrate the architecture of the Mesozoic and Paleozoic sequences beneath the molasse basin fill (Figure 3). Note that the section is flattened on top of the Mesozoic sequence with a vertical exaggeration of 8x. The Porrau “diabase complex” is shown in a simplified manner associated with a folded structure which may be seen as a positively inverted flank of a Jurassic half-graben (Figure 2). The progressive truncation of the Jurassic and Cretaceous units beneath the base molasse unconformity (Figure 3) indeed suggests an inversional episode with considerable strata (up to 1–2 km?) eroded between the Cretaceous and the Late Oligocene (Egerian) over the Altenmarkt half-graben.

### Data and methodology used

The present study was focused on the Porrau-2 well as it had a relatively large number of cores in the inferred Mesozoic part of it (Figure 3) with generally very good (>90%) recovery rates. As an illustration of this, the photos of two of the core boxes here (Figure 6) show examples of the metadolerite and dacite which were the focus of our analysis.

For the study, 12 core samples were selected at OMV’s core facility in Gänsendorf (Table I). These samples were selected to represent both the intrusive subvolcanic rocks and the siliciclastic host rocks. However, the present paper focuses on the magmatics and the results on the clastic rocks will be published elsewhere.

The 12 samples from the well Porrau-2 were investigated by means of petrographic,





**Figure 6.** Cores of the metabasalt of Sample 2 (left) and dacite of Sample 5 (right) in the Porrau-2 well drilled by OMV in Lower Austria in 1960/61. Note the generally very good (>90%) recovery of the core material. The core boxes are 1 m long, the deepest part of the core at the upper right-hand corner in Box #1  
**6. ábra.** Az OMV által 1960/61-ben Alsó-Ausztriában, a Porrau-2 kútban fűrt metabazalt (2. minta, balra) és dácit (5. minta, jobbra) magjai. A magkihozatal általában >90%-os volt. A magládák 1 m hosszúak, a mag legmélyebb része a jobb felső sarokban, az 1. dobozban található

XRD, and XRF analyses. In this contribution we included only the description of the subvolcanic rocks. Below is the list of the selected samples from well Porrau-2 (marked in red). For a description of both the XRD and XRF analysis methodology used in this study, please see SPRÁNITZ et al. (this issue).

**Table I.** Sample listing of the Porrau-2 well. Note the different type of rocks acquired. The current study focuses on the subvolcanic intervals and a follow-up study will integrate the sandstone petrology as well

**I. táblázat.** A Porrau-2 kút mintáinak listája. A mintázás során szubvulkáni és üledékes kőzeteket is vettünk, amelyek közül jelen munka csak a szubvulkáni kőzetekre fókuszál. Az üledékes kőzeteket egy későbbi tanulmányban dolgozzuk fel

| Sample # | Top depth (m) | Bottom depth (m) | Core # | Box # | lithology |
|----------|---------------|------------------|--------|-------|-----------|
| 1        | 1816,6        | 1821,4           | 27     | 1     | volcanic  |
| 2        | 1849,8        | 1855,5           | 29     | 6     | volcanic  |
| 3        | 1870,2        | 1875,6           | 30     | 3     | sandstone |
| 4        | 1891          | 1898             | 31     | 4     | volcanic  |
| 5        | 1930,6        | 1937             | 33     | 2     | volcanic  |
| 6        | 1973,6        | 1980,5           | 35     | 6     | sandstone |
| 7        | 1973,6        | 1980,5           | 35     | 3     | volcanic  |
| 8        | 1992,3        | 1998,5           | 36     | 1     | sandstone |
| 9        | 1758,6        | 1762,4           | 22     | 1     | sandstone |
| 10       | 1772          | 1774,35          | 24     | 1     | volcanic  |
| 11       | 1805,3        | 1812,3           | 26     | 6     | volcanic  |
| 12       | 1805,3        | 1812,3           | 26     | 2     | sandstone |

In addition to the petrographic analysis, three samples were selected for K-Ar dating which was carried out at the Institute for Nuclear Research (ATOMKI), Hungary. One sample was selected for detrital zircon (U-Th)/He and U-Pb geochronology analysis which was performed by the University of Ottawa, Canada. A brief description of all the age dating methods is given below.

#### Geochemistry based on XRD and XRF (X-ray Fluorescence Analysis)

X-ray fluorescence (XRF) is a method of X-ray spectroscopy used for qualitative and especially for the quantitative determination of elements. By using the method, liquid, powder, or compact samples can be measured. It works non-destructively and is largely independent of the bonding state of the elements. The elemental analysis is determined using a Analytical EPSILON 3 XL Energy-dispersive X-ray fluorescence spectrometer (Ag radiation with software-controlled maximum 50 kV, maximum 3 mA and 15 W tube power). The Epsilon 3 software program is used for qualitative and quantitative analyses, and this include Omnian software module for standardless and fingerprint applications. Geochemical investigation of volcanic rocks is a power-



ful tool supporting petrographic observations and enables to classify volcanic rocks based on elementary composition.

#### *K-Ar age dating*

The radiometric geochronology analysis, using the Cassinot-Gillot K/Ar dating method, was carried out in Geochronology Lab of the HUN-REN ATOMKI, at the Institute for Nuclear Research in Debrecen, Hungary. Based on the petrography, samples were crushed and sieved to typically 63–125 and 125–250  $\mu\text{m}$ . The selected grain size fraction was washed with deionized water and a 10 V/V% acetic acid solution was used to remove the carbonate content of the samples. The magnetic fraction was separated by a Frantz magnetic separator. Heavy liquid (sodium poly-tungstate: SPT) set to 2.72 and 2.88  $\text{g}/\text{cm}^3$  was used to isolate ground-mass and minerals fractions (e.g., plagioclase, biotite).

The separated fractions were analysed by the non-spiked K-Ar method (CASSIGNOL & GILLOT 1982, GILLOT & CORNETTE 1986) following the procedure of the Geochronology Lab of the Institute for Nuclear Research, Debrecen. The potassium content was measured on 50 mg sample aliquots, after dissolution by HF and HNO<sub>3</sub>, with a Sherwood-400-type flame spectra-photometer with accuracy better than  $\pm 1.5\%$ . Separated mineral sample splits were subjected to heating at 100 °C for 24 h under vacuum to remove atmospheric Ar contamination that was adsorbed on the surface of the mineral particles during sample preparation. Argon was extracted from the minerals by fusing the samples with high-frequency induction heating at 1300 °C. Released gases were cleaned in two steps in a low-blank vacuum system by hot (350° and 250° C) St-101 and St-707 SAES getters operated at room temperature. Isotopic composition of the Ar was measured by a MAP-215-50 noble gas mass spectrometer, following the non-spiked method of GILLOT & CORNETTE (1986), and corrected for the atmospheric <sup>40</sup>Ar/<sup>36</sup>Ar ratios. The calibration of our <sup>40</sup>Ar signal is checked routinely using analyses of the HD-B1 (HESS & LIPPOLT 1994, SCHWARZ & TRIELOFF 2007), GL-O (ODIN et al. 1982) international standards. During this study, analyses of HD-B1 yielded an age of 24.29 $\pm$ 0.34 Ma, which compares well with the recommended values of 24.21 $\pm$ 0.32 Ma. Standard GL-O yielded 95.26 $\pm$ 1.35 Ma, which differs only insignificantly from the reported age (95.03 $\pm$ 1.11 Ma). Decay constants recommended by STEIGER & JÄGER (1977) were used for the age calculation, with an overall error of  $\pm 1\%$ . An error of the samples was calculated using the equation of QUIDELLEUR et al. (2001).

#### *Detrital zircon U-Pb geochronology*

After crushing of a coarse-grained sandstone from 1819 m depth, the 63-250  $\mu\text{m}$  size fraction was rinsed through a decantation process, and heavy mineral separation was then conducted using methylene iodide (SG: 3.0  $\text{g}/\text{cm}^3$ ) in order to obtain a more concentrated fraction of zircon. The heavy mineral separates were then individually passed through a

Frantz magnetic mineral separator as needed to further isolate zircon. Individual zircon grains were then picked using tweezers under a binocular microscope.

Zircon for laser ablation inductively coupled plasma mass spectrometry (LA ICP-MS) U-Pb analysis were mounted in epoxy and polished for imaging. A JEOL 6610LV Scanning Electron Microscope (SEM; University of Ottawa, Canada) was used to characterize the zircon and to identify the internal structure of the mineral or rim overgrowths on the zircon using cathodoluminescence imaging. A Resonetics M-50 193 nm ArF Excimer laser ablation system coupled to an Agilent 7700x quadrupole ICP-MS system (University of Ottawa, Canada) was utilized for the zircon U-Pb analyses, following the protocol of MCFARLANE & LUO (2012) and the common lead correction of ANDERSEN (2002). Single spot analyses were completed with the laser operated at a repetition rate of 6 Hz, spot size of 32  $\mu\text{m}$ , and pulse energy of 4.72 J/cm<sup>2</sup>. Reference material 91500 zircon (U-Pb: 1065.4 $\pm$ 0.3 Ma; WIEDENBECK et al. 1995) was analyzed as a standard under the same conditions as the unknowns. A secondary standard, Plešovice zircon (U-Pb: 337.1 $\pm$ 0.4 Ma; SLÁMA et al. 2008), was also used to correct for analytical drift. All data was reduced, and drift corrected using Glitter v4.4.4, with reference material uncertainty calibrated to 1%. The final corrected data were plotted using IsoplotR (VERMEESCH 2018).

#### *Detrital zircon (U-Th)/He geochronology*

The analytical portion of the (U-Th)/He experiments was conducted at the TRaIL (Thermochronology Research and Instrumentation Laboratory) facility at the University of Colorado (Boulder, USA). Individual mineral grains are placed into small Nb tubes that are then crimped on both ends. This Nb packet is then loaded into an ASI Alphachron He extraction and measurement line. The packet is placed in the UHV extraction line ( $\sim 3 \times 10^{-8}$  torr) and heated with a diode laser to  $\sim 800$ – $1100$  °C for 5 to 10 m to extract the radiogenic <sup>4</sup>He. The degassed <sup>4</sup>He is then spiked with approximately 13 ncc of pure <sup>3</sup>He, cleaned via interaction with two SAES getters, and analyzed on a Balzers PrismaPlus QME 220 quadrupole mass spectrometer. Degassed grains are then removed from the line and taken to a Class 10 clean lab for dissolution. Zircon are dissolved using Parr large-capacity dissolution vessels in a multi-step acid-vapor dissolution process. Grains (including the Nb tube) are placed in Ludwig-style Savillex vials, spiked with a <sup>235</sup>U-<sup>230</sup>Th tracer, and mixed with 200  $\mu\text{l}$  of Optima grade HF. The vials are then capped, stacked in a 125 mL Teflon liner, placed in a Parr dissolution vessel, and baked at 220 °C for 72 h. After cooling, the vials are uncapped and dried down on a 90 °C hot plate until dry. The vials then undergo a second round of acid-vapor dissolution, this time with 200  $\mu\text{l}$  of Optima grade HCl in each vial that is baked at 200 °C for 24 h. Vials are then dried down a second time on a hot plate. Once dry, 200  $\mu\text{l}$  of a 7:1 HNO<sub>3</sub>:HF mixture is added to each vial, the vial is capped, and cooked on the hot plate at 90 °C for 4 h.

Once the minerals are dissolved, regardless of the dissolution process, they are diluted with 1 to 3 mL of doubly-deionized water, and taken to the ICP-MS lab for analysis. Mineral standards of Durango apatite (31.5 Ma) and Fish Canyon Tuff zircon (28.2 Ma) are routinely analyzed (degassed and dissolved) in conjunction with the samples with each run to ensure data integrity. Sample solutions, along with standards and blanks, are analyzed for U, Th, and Sm content using a Thermo Element 2 magnetic sector mass spectrometer. Once the U, Th, and Sm contents have been measured, He dates and all associated data are calculated on a custom spreadsheet made by TRAIL staff.

### Analytical results on the volcanic samples

The methods described above derived several new results to formulate a new, but still preliminary interpretation of the sills penetrated in the Porrau-2 well. Six of the seven volcanic samples were classified as metadolerites based on petrographic observations (see below) supplemented by XRD and XRF data (*Tables II and III*). The metadolerite samples are highly altered based on macroscopic and microscopic observations (*Figures 6, 7, 8*), as are all the other sills in the Porrau-2 hole (*Figure 5*). Primary minerals such as plagioclase and mafic minerals have been intensely replaced by secondary minerals such as chlorite, epidote and calcite. However, some of the moderately altered samples retained some amphiboles and biotite and therefore were selected for K-Ar dating (see below). One of the samples (#5) is a more acidic volcanic rock type compared to the metadolerites and it is classified as a dacite (*Figure 8*).

#### *Metadolerite*

The textures of the suite are variable, but most of the rocks have characteristics of mafic subvolcanic sills (*Figures 7, 8*). Porphyritic texture is visible both macroscopically and microscopically on some of the samples. Phenocrysts are dominated by plagioclase and rarely by chlorite pseudomorphs after pyroxene. Although no pyroxene was found in the samples, the outlines of the chlorite pseudomorphs suggest pyroxene precursors. The plagioclase laths in the groundmass are mostly in contact and the interstitial space is filled with either chlorite or opaque minerals, showing the intergranular texture. The plagioclase is in some cases partially enveloped by chlorite pseudomorphs, which is characteristic for the subophitic texture. The change from intergranular to subophitic to ophitic textures in basaltic rocks results from slower cooling and slower crystallization rates. This textural sequence is typically found from the margins towards the center in doleritic rocks (basaltic dikes). Correspondingly, the crystal size increases from the margins towards the center.

Plagioclase phenocrysts are medium to coarse grained. The plagioclase in the groundmass is mostly fine to rarely medium grained. Crystals are euhedral and phenocrysts are

often zoned. Chlorite usually occurs as pseudomorphs after pyroxene. It often replaces some or all of the biotite and hornblende. Opaque minerals are the primary minerals of dolerites and are dominated by ilmenite and minor magnetite. The ilmenites are often rimmed by leucoxene, which allows ilmenite to be distinguished from magnetite and other iron-titanium oxides. Unaltered ilmenite and rare magnetite form euhedral crystals that are 30 to 100  $\mu\text{m}$  in size. Ilmenite in some samples is completely altered to leucoxene, a fine-grained alteration product of titanium minerals. Occasionally titanite was observed. Leucoxene occurs mainly either as an alteration product of ilmenite or associated with chlorite pseudomorphs after pyroxene. Apatite is a secondary mineral that forms acicular prisms between 3 and 13  $\mu\text{m}$  in diameter. The basal sections are hexagonal in shape. The apatite crystals are mainly found as inclusions in other minerals. Biotite is a secondary mineral occurring in the groundmass as euhedral platelets. Hornblende occurs in the groundmass as euhedral prisms. The basal sections show characteristic 124-56° cleavage intersections. The hornblende is partly replaced by chlorite. Epidote is a common to rare secondary replacement mineral, occurring in association with chlorite pseudomorphs or replacing the host rock in general. Rare clinozoisite has also been observed. The degree of epidotization varies from intense in some samples to virtually absent in others.

Rarely, epidote also heals fractures. Epidote also occurs as inclusions in plagioclase and results from saussuritization. Quartz is a secondary mineral that occurs as idiomorphic megaquartz. Quartz is found exclusively in dissolution vuggy pores. The idiomorphic quartz crystals are surrounded by blocky calcite, indicating that the latter is post-dating the former. Quartz also occurs in rounded patches, or ocelli, in which there has been progressive crystallization from the margins towards the center. Calcite is a secondary alteration mineral that occurs mostly as a pore-filling blocky cement. The calcite is found in certain samples within vuggy pores together with euhedral megaquartz, which is post-dating the latter. The vuggy pores are indicative of dissolution of the groundmass and phenocrysts. The calcite sometimes occurs within the chlorite pseudomorphs after pyroxene, replacing the chlorite. This suggests chlorite dissolution. Crosscutting fractures in the host rock are mainly cemented by blocky calcite.

#### *Dacite*

Importantly, one of the samples (#5) is a more acidic subvolcanic/magmatic rock type than metadolerite and is classified as a dacite (*Figure 8*). The texture is porphyritic, characterized by large plagioclase phenocrysts, quartz phenocrysts with characteristic embayment and ghosts of former mafic phenocrysts. The phenocrysts are up to 1.3 mm in size. The groundmass is composed of fine-grained plagioclase laths, quartz, and secondary replacement minerals. The plagioclase in the groundmass and in the phenocrysts is extensively replaced by sericite, chlorite and calcite.



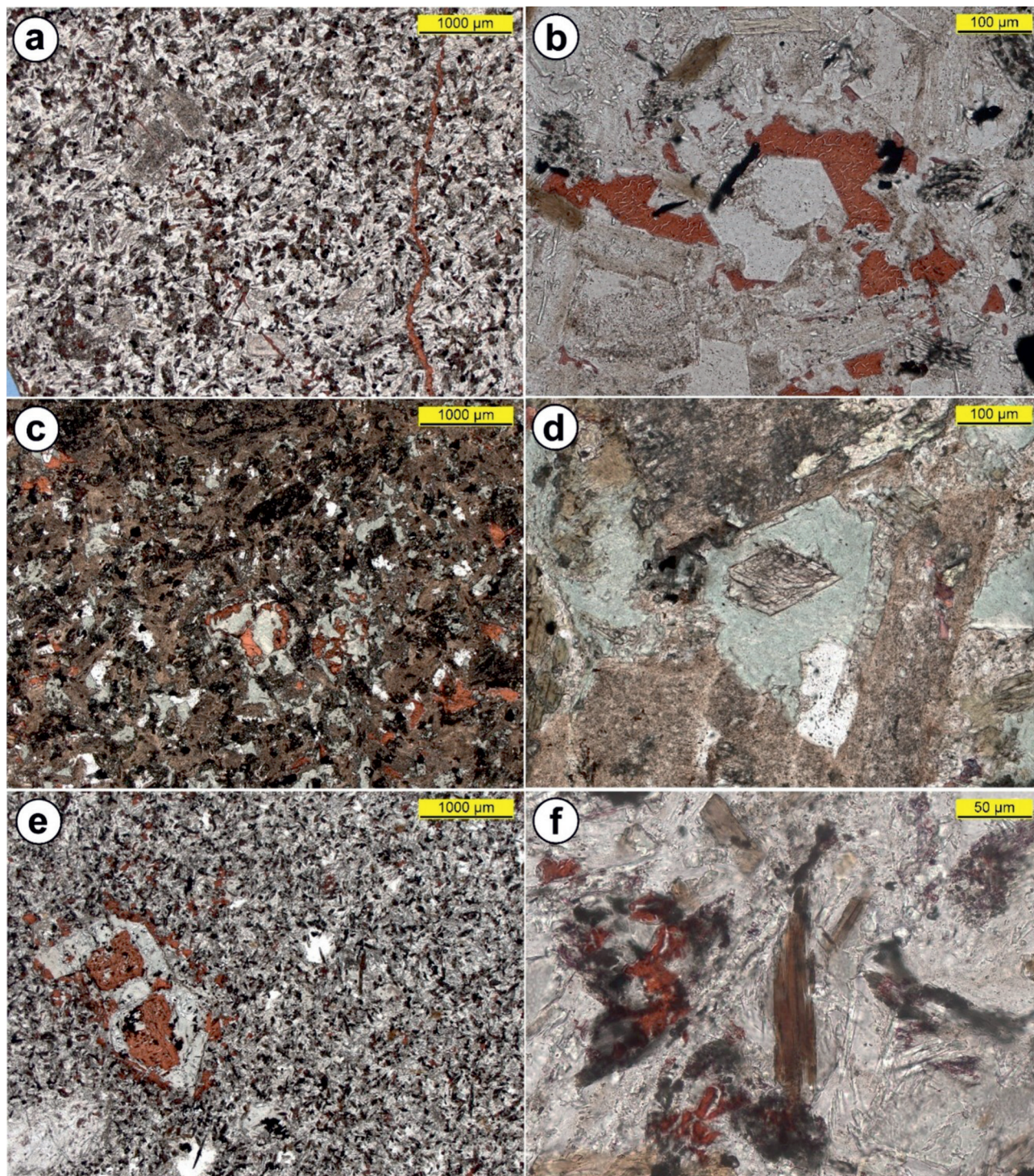


**Figure 7.** Thin section photomicrographs of different sub-volcanic levels in the Porrau-2 borehole. a) Fine-grained metadolerite with fine-grained plagioclase phenocrysts and intergranular texture. Sample 1. b) Close-up of sample 1: intergranular texture with a former vug filled with idiomorphic megaquartz followed by pore-filling blocky calcite cement. c) Fine- to medium-grained porphyritic metadolerite with partly subophitic texture. The plagioclase is brownish due to abundant inclusions. Greenish chlorite pseudomorphs replace mafic minerals. Sample 2. d) Close-up of sample 2: the core of this amphibole has not been consumed by chloritisation. e) Fine-grained porphyritic dolerite with intergranular texture. The large phenocrysts are chlorite and calcite pseudomorphs after mafic minerals and plagioclase. The white dots represent the quartz ocelli. Sample 4. f) Enlarged view of sample 4: in the centre brownish biotite with chloritised rims

**7. ábra.** A Porrau-2 fúrás különböző szubvulkáni szintjeinek vékonycsiszolatos mikroszkópos felvételei. a) Finomszemcsés metadolerit, finomszemcsés plagioklász fenokristályokkal és intergranuláris textúrával. 1. minta. b) Az 1. minta nagyobb nagyításban: intergranuláris szövet egy idiomorf megakvarccal kitöltött, korábbi üreggel, amelyet porustöltő, tömbös kalcitcement követ. c) Finom- és közepszemcsés porfirites metadolerit részben szubofitos szövettel. A plagioklász a sok zárvány miatt barnás színű. A mafikus ásványokat zöldes színű kloritpszeudomorfok helyettesítik. 2. minta. d) A 2. Minta nagyobb nagyításban: ennek az amfibolnak a magját nem emésztette fel a kloritizáció. e) Finomszemcsés porfirites dolerit intergranuláris textúrával. A nagy fenokristályok mafikus ásványok, valamint plagioklász után klorit és kalcit pszeudomorfok. A fehér pöttyök a kvarc-ocellumokat jelölik. 4. minta. f) A 4. minta nagyított nézete: középen barnás biotit kloritosodott peremmel



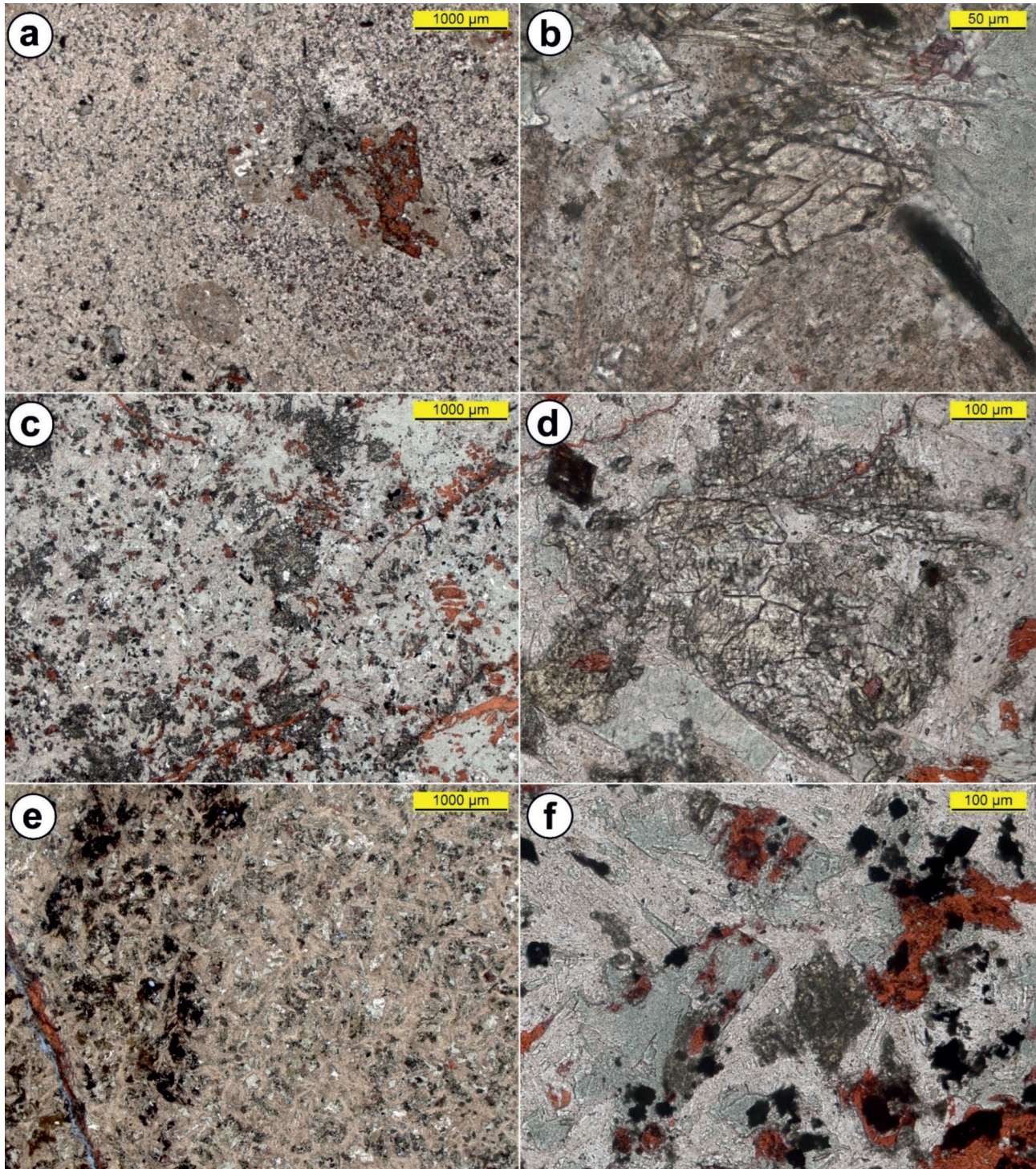


**Figure 8.** Thin section photomicrographs of different subvolcanic levels in the Porrau-2 borehole. a) Porphyritic dacite with large plagioclase phenocrysts. Sample 5. b) Close-up of sample 5: in the centre is a basal section of an amphibole. c) Fine- to medium-grained porphyritic metadolerite with plagioclase phenocrysts. The sample is strongly chloritised and calcitised. Sample 7. d) Close-up of sample 7: plagioclase is almost completely replaced by epidote (yellowish). e) Heavily altered metadolerite with subophitic texture. The plagioclase is brownish due to abundant inclusions. Sample 10. f) Subophitic texture: plagioclase laths are partly enclosed by pseudomorphs after pyroxene. The pseudomorphs consist of chlorite, calcite, leucoxene and epidote. Sample 11. Note that all the thin-sections analysed show a consistent subvolcanic signature

**8. ábra.** A Porrau-2 fúrás különböző szubvulkáni szintjeinek vékonycsiszolatos mikroszkópos felvételei. a) Porfirites dácit nagy plagioklász fenokristályokkal. Az 5. minta. b) Az 5. minta nagyítása: középen egy amfibol bazális metszete. c) Finom- és közepeszemcsés porfirites metadolerit plagioklász fenokristályokkal. A minta erősen kloritosodott és kalcitosodott. A 7. minta. d) A 7. minta nagyítása: a plagioklász szinte teljesen felváltotta az epidot (sárgás). e) Erősen módosult metadolerit szubofitos szövettel. A plagioklász a sok zárvány miatt barnás színű. 10. minta. f) Szubofitos szövet: a plagioklász léceket részben piroxén utáni pszeudomorfok veszik körül. A pszeudomorfok kloritból, kalcitból, leukoxénből és epidotból állnak. 11. minta. Megjegyzendő, hogy az összes elemzett vékonycsiszolat következetes szubvulkáni jellegzetességet mutat



Chlorite is present as small crystals in the groundmass. The host minerals were fine-grained mafic minerals as part of the groundmass. Ghosts of mafic phenocrysts are also completely replaced by chlorite and calcite pseudomorphs. Some of these have hexagonal basal sections, suggesting that the phenocrysts were amphiboles. Apatite forms acicular prisms. The euhedral opaque minerals range in size from 50 to 100  $\mu\text{m}$ . They have been completely replaced by granular leucoxene, suggesting an ilmenite host mineral. Blocky calcite cement replaces groundmass, plagioclase phenocrysts and forms pseudomorphs with chlorite after mafic phenocrysts. Calcite also heals micro-fractures. There is no evidence for devitrification of volcanic glass, therefore we suggest that the dacite is also intrusive in character.

#### *Autometamorphic processes based on thin-section analysis*

The subvolcanic rocks in Porrau-2 well are intensively replaced by secondary minerals. As noted by WIESENER (1965), the country rock shows no signs of metamorphism, so the only way the secondary minerals could have formed in the intrusion is by autometamorphism. The autometamorphic processes are more common in plutonic or subvolcanic rocks because they remain at elevated temperatures for a longer time than purely extrusive volcanic rocks, making the subvolcanic rocks more susceptible to autometamorphic alteration. The reactions are deuteric and involve water as the rock cools.

The hornblende is present in a single sample of coarser crystal size from a more central part of the intrusion. We consider hornblende to be a secondary alteration mineral from trough unroofing of primary pyroxenes. Biotite also most likely resulted from alteration of pyroxene or amphibole. Both alteration processes occurred relatively early at higher temperatures compared to later processes discussed below.

Chloritization is the most widespread alteration process, affecting all samples examined. Chlorite mainly replaced the mafic suite of minerals. The pyroxenes were all lost and even the hornblende and biotite were partially replaced. Chloritization is not restricted to the mafic minerals as it also partially replaced plagioclase. The latter has also been replaced by several other minerals. Sericitization is one of the most common alterations of plagioclase, where very fine-grained white mica (muscovite or paragonite), commonly known as sericite, replaces the plagioclase host rock. Epidote is also present in a few samples and replaces plagioclase. We attribute its formation to saussurization. A very common process is the alteration of ilmenite to leucoxene.

Quartz is characterized by euhedral crystal faces and is surrounded by calcite cement, indicating that it precipitated in an open pore space prior to calcite cement. Calcite replacement is interpreted to be the final stage of the alteration process, in which all primary minerals are partially replaced. The host rock is fractured, and the fractures cement-

ed by calcite, indicating that precipitation occurred in the brittle regime after the intrusion had solidified.

#### *Geochemistry based on XRD and XRF (X-ray Fluorescence Analysis)*

Based on the XRF results (*Table II*) we used the Total Alkali-Silica (TAS) diagram (LE BAS et al. 1986) for classification of volcanic rocks (*Figure 9a*). X-axis represents the silica contents whereas Y-axis shows the value of alkaline components. The TAS diagram of the studied seven volcanic samples shows six of the seven measured samples have low silica contents and plot in the basalt and trachy-basalt field (*Figure 9a*). Interestingly, there is an outlier sample which is a dacite based on its composition (Sample 5).

The AFM diagram (*Figure 9b*) adopted from VERMEESCH & PEASE (2021) shows the same overall grouping of all the igneous samples in the basalt domain except for a dacite sample. Also, all the samples plot closer to the calc-alkaline Bowen trend than to the tholeiitic Fenner trend.

The XRF results (*Table II*) were also used to determine the igneous series of the subvolcanic rocks. The AFM diagram was used to plot the  $\text{Fe}_2\text{O}_3$ , MgO and  $\text{K}_2\text{O}+\text{Na}_2\text{O}$  contents of the samples. The diagram (*Figure 9b*) shows that the samples fall into the calc-alkaline trend. Calc-alkaline rocks are typically found in volcanic arcs above subduction zones, often in island arcs, and especially in arcs developed over continental crust.

#### *K-Ar age results*

The dated samples included (with their OMV/ATOMKI sample numbers) two metadolerite (sample 1/9034, from 1816–1821 m; sample 2/9035, from 1849–1855 m) and a dacite (sample 5/9036, from 1930–1937 m).

The analytical data and calculated ages are summarized in *Table IV* and *Figure 10*. The amount of radiogenic Ar of the samples was very high,  $^{40}\text{Ar}_{\text{rad}}$  (%) was between 73% and 95%. The two biotite-rich fractions from No. 9034 sample have high potassium content (3.0–3.9%) and have younger, Hauterivian to Valanginian ages ( $135.9\pm 2.4$  and  $141.2\pm 2.5$  Ma). The light groundmass fraction yielded a much older age ( $231.8\pm 4.0$  Ma). The sample No. 9035 is characterized by lower potassium (0.5–2.2%) and older age population ( $243.8\pm 4.8$ – $268.4\pm 5.2$  Ma; Triassic–Permian), respectively.

The dacite sample (No. 9036), provided the oldest ages ( $283.2\pm 5.1$  Ma –  $284.4\pm 5.0$  Ma).

#### **Discussion**

For geologic age data interpretation, we relied on three separate methods such as K-Ar, detrital zircon U-Pb and (U-Th)/He geochronology. A tentative interpretation of all these data sets is summarized below highlighting the need for additional analysis.

**Table II.** X-ray fluorescence spectrometry results only of the subvolcanic samples in the Porrau-2 well*II. táblázat.* A Porrau-2 fűrés szubvulkáni mintáin végzett röntgenfluoreszcens spektrometriás vizsgálatok eredménye

| Sample ID                      | 1             | 2             | 4             | 5             | 7             | 10             | 11            |
|--------------------------------|---------------|---------------|---------------|---------------|---------------|----------------|---------------|
| Comp. (wt.%) / Depth (m)       | 1816.6-1821.4 | 1849.8-1855.5 | 1891.0-1898.0 | 1930.6-1937.0 | 1973.6-1980.5 | 1772.0-1774.35 | 1805.3-1812.3 |
| Na <sub>2</sub> O              | 1,92          | 3,98          | 2,46          | 4,54          | 2,73          | 3,59           | 3,80          |
| MgO                            | 6,28          | 8,97          | 6,88          | 1,13          | 8,86          | 12,28          | 7,93          |
| Al <sub>2</sub> O <sub>3</sub> | 16,73         | 16,93         | 19,90         | 18,40         | 16,82         | 18,24          | 17,95         |
| SiO <sub>2</sub>               | 46,64         | 49,51         | 47,80         | 65,69         | 45,46         | 45,99          | 46,84         |
| P <sub>2</sub> O <sub>5</sub>  | 0,00          | 0,00          | 0,66          | 0,00          | 0,00          | 0,60           | 0,48          |
| K <sub>2</sub> O               | 3,05          | 1,36          | 1,00          | 2,03          | 1,34          | 0,32           | 0,96          |
| SO <sub>3</sub>                | 0,06          | 0,10          | 0,36          | 0,02          | 0,12          | 0,01           | 0,11          |
| CaO                            | 14,78         | 9,13          | 8,23          | 4,26          | 14,20         | 4,04           | 9,38          |
| MnO                            | 0,16          | 0,11          | 0,16          | 0,06          | 0,16          | 0,17           | 0,11          |
| Fe <sub>2</sub> O <sub>3</sub> | 9,23          | 8,95          | 11,17         | 3,44          | 9,20          | 13,12          | 11,10         |
| Cl                             | 0,10          | 0,11          | 0,09          | 0,11          | 0,10          | 0,16           | 0,08          |
| Ti                             | 0,85          | 0,67          | 1,14          | 0,24          | 0,78          | 1,32           | 1,01          |
| Cr                             | 0,01          | 0,03          | 0,02          | 0,03          | 0,02          | 0,01           | 0,02          |
| Ni                             | 0,00          | 0,01          | 0,01          | 0,01          | 0,01          | 0,01           | 0,01          |
| Zn                             | 0,01          | 0,01          | 0,01          | 0,01          | 0,01          | 0,02           | 0,02          |
| Sr                             | 0,07          | 0,06          | 0,04          | 0,02          | 0,09          | 0,07           | 0,11          |
| Zr                             | 0,02          | 0,02          | 0,03          | 0,02          | 0,02          | 0,02           | 0,02          |
| V                              | 0,02          | 0,02          | 0,02          | 0,00          | 0,02          | 0,03           | 0,03          |
| Ba                             | 0,07          | 0,03          | 0,02          | 0,00          | 0,06          | 0,00           | 0,04          |

### *Interpretation of the K-Ar age determination results*

Our study is providing the first radiometric age dating of the various subvolcanic units encountered in the Porrau-2 well. A mafic mineral and two groundmass mineral fractions separated from the metadolerite (no. 9035) taken from lower level of the magmatic sequence yielded discordant Triassic and Permian ages (mafic: 9035a 243.8±4.8 Ma; gm 9035c 254.89±4.8 Ma; 9035d 268.4±5.2 Ma). Based on the geological data available for the emplacement of this meta-

dolerite, a much younger, Late Jurassic (c. 165–145 Ma) age was expected for the intrusives emplaced in a Middle Jurassic sequence (WIESENER 1965). There are various options for the interpretation of these analytical data:

(1) These ages can be considered as “mixing ages” – due to the incorporation of excess Ar. Sources of excess Ar can be: (a) Xenoliths or xenocrysts from the footwall, incorporated in the sample. It is unlikely, however, as the samples were carefully selected and treated. (b) Hydrothermal overprint of the samples during a hydrothermal or tectonothermal event. All the samples have oriented texture and many of

**Table III.** XRD bulk mineralogy analysis results on all 12 core samples in the Porrau-2 well*III. táblázat.* A Porrau-2 fűrés mind a 12 magmintájának XRD ásványtani elemzési eredményei

| Nr. | Well     | Depth (m)      | Quartz | Albite | Anorthite | Calcite | Ankerite | Microcline | Anhydrite | Orthoclase | Chlorite | Hornblende | Chamosite | Epidote | Clay Tot+Mica |
|-----|----------|----------------|--------|--------|-----------|---------|----------|------------|-----------|------------|----------|------------|-----------|---------|---------------|
| 1   | Porrau 2 | 1816,6-1821,4  | 9,78   | 4,64   | 23,88     | 15,62   |          |            |           | 13,19      | 29,32    |            |           |         | 3,57          |
| 2   | Porrau 2 | 1849,8-1855,5  | 5,67   | 31,5   |           | 5,89    |          | 12,78      |           |            | 21,11    | 5,57       |           | 15,62   | 1,86          |
| 3   | Porrau 2 | 1870,2-1875,6  | 55,47  | 22,01  |           | 4,64    |          |            | 1,71      |            | 16,12    |            |           |         | 0,05          |
| 4   | Porrau 2 | 1891,0-1898,0  | 11,53  | 13,33  | 23,47     | 12,76   |          |            |           |            | 36,3     |            |           |         | 2,61          |
| 5   | Porrau 2 | 1930,6-1937,0  | 30,41  | 33,13  |           | 5,85    |          |            |           |            | 10,67    |            |           |         | 19,94         |
| 6   | Porrau 2 | 1973,6-1980,5  | 58,33  | 14,27  |           | 0,19    |          |            |           |            | 6,7      |            |           |         | 20,51         |
| 7   | Porrau 2 | 1973,6-1980,5  | 12,13  | 31,37  |           | 7,59    | 0,28     |            |           |            | 37,43    |            |           |         | 11,2          |
| 8   | Porrau 2 | 1992,3-1998,5  | 22,68  | 20,67  |           | 8,59    |          |            |           |            |          |            | 7,78      |         | 40,28         |
| 9   | Porrau 2 | 1758,6-1762,4  | 61,87  | 23,11  |           |         |          |            |           |            | 14,96    |            |           |         | 0,06          |
| 10  | Porrau 2 | 1772,0-1774,35 | 7,69   | 54,43  |           | 5,87    |          |            |           |            |          |            | 15,5      |         | 16,51         |
| 11  | Porrau 2 | 1805,3-1812,3  | 8,57   | 32,66  |           | 9,43    |          |            |           |            | 39,53    |            |           |         | 9,81          |
| 12  | Porrau 2 | 1805,3-1812,3  | 69,01  | 17,22  |           |         |          |            |           |            | 13,72    |            |           |         | 0,05          |



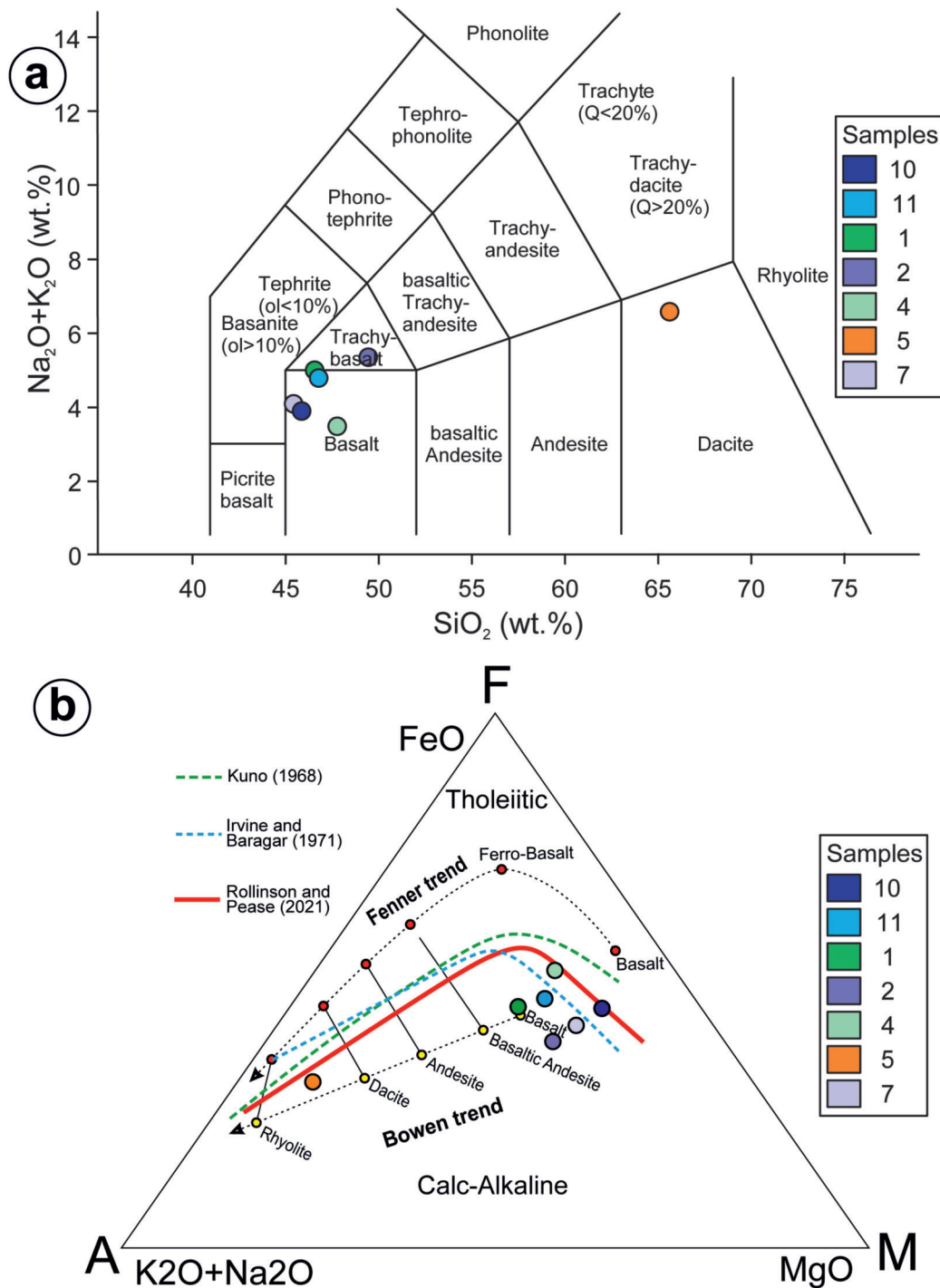


**Figure 9.** a) Total Alkali-Silica (TAS) diagram (LE BAS et al. 1986) of the analyzed seven volcanic rocks. b) AFM diagram (VERMEESCH & PEASE 2021) with discrimination boundaries between the tholeiitic (following the Fenner trend) and calc-alkaline (following the Bowen trend) igneous suites

**9. ábra.** a) A 7 vizsgált vulkáni kőzet összalkáli- és  $\text{SiO}_2$  (TAS) diagramja (LE BAS et al. 1986). b) AFM-diagram (VERMEESCH & PEASE 2021) a tholeiites (a Fenner-trendet követő) és a mészalkáli (a Bowen-trendet követő) vulkáni sorozatok közötti megkülönböztető határokkal

the minerals are altered, indicating that the samples were affected by secondary processes. These thermal events could have opened the lattice of the minerals and disturb the radiometric clock of the samples. (c) Diffusion of Ar from the Carboniferous footwall lithology (Figures 3, 4) into the sills. Diffusion of Ar depends on the temperature, but it is

spatially very limited (typically a few meters), therefore the footwall must be proximal to the volcanics. Given that metadolerites are characteristically thin, i.e. on the order of a few meters, this scenario is highly probable. The diffusion model is further supported by the ages of the various mineral fractions: biotite, that has the highest closure temperature

Table IV. K-Ar analytical data obtained on dacite and metadolerite samples

IV. táblázat. Dácit és metabazalt mintákon kapott K-Ar analitikai adatok

| Sample #                                 | Lab code | Sample                 |        | K [%] | <sup>40</sup> Ar <sub>rad</sub> [ccSTP/g] | <sup>40</sup> Ar <sub>rad</sub> [%] | Age [Ma]      | σ [Ma] |
|--|----------|------------------------|--------|-------|---|-------------------------------------|---------------|--------|
| <b>Porrau-2 1816-1821 m metadolerite</b> |          |                        |        |       |   |                                     |               |        |
| 1  | 9034a    | gm 1 (biotite rich)    | ρ>2.72 | 3.91  | 2.230E-05                                 | 95.5                                | <b>141.21</b> | 2.47   |
| 2  | 9034b    | gm 2 (feldspar rich)   | ρ<2.72 | 2.06  | 1.981E-05                                 | 96.4                                | <b>231.78</b> | 4.04   |
| 3  | 9034c    | gm 2 (biotite rich)    | ρ>2.72 | 2.99  | 1.640E-05                                 | 96.6                                | <b>135.9</b>  | 2.37   |
| <b>Porrau-2 1849-1855 m metadolerite</b> |          |                        |        |       |   |                                     |               |        |
| 4  | 9035a    | mafic                  | ρ>2.88 | 0.54  | 5.458E-06                                 | 73.2                                | <b>243.76</b> | 4.76   |
| 5  | 9035c    | gm (light)             | ρ<2.72 | 1.05  | 1.182E-05                                 | 75.0                                | <b>268.38</b> | 5.20   |
| 6  | 9035d    | gm (heavy)             | ρ>2.72 | 1.80  | 1.922E-05                                 | 80.4                                | <b>254.89</b> | 4.78   |
| <b>Porrau-2 1930-1937 m dacite</b>       |          |                        |        |       |   |                                     |               |        |
| 7  | 9036a    | feldspar (plagioclase) | ρ<2.72 | 1.32  | 1.577E-05                                 | 87.8                                | <b>283.21</b> | 5.11   |
| 8  | 9036b    | mafic (amphibole)      | ρ>2.88 | 2.23  | 2.670E-05                                 | 96.1                                | <b>284.37</b> | 4.97   |

(250–350 °C) approaches the expected age. Plagioclase, with a lower closure temperature (150–250 °C) is much more sensitive to secondary processes and, therefore, it provided older, probably mixed ages.

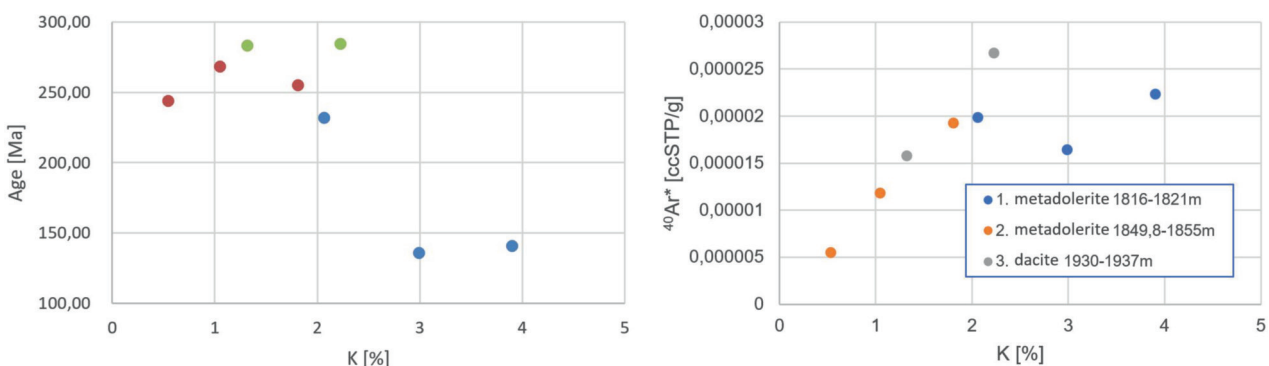
(2) The older Permian geological age of the metadolerite is impossible to explain, if these sills were indeed emplaced in a Jurassic sequence.

The radiometric ages 283.2±5.1 Ma and 284.4±5.0 Ma measured on different mineral fractions of the dacite are within error and indicate an Early Permian age. If the rock is indeed a sill with dacitic composition, these identical dates may represent the geological age of the rock emplaced in a pre-Permian rock. It should be also noted, that post-Variscan, Permian acidic intrusions intruding Carboniferous shales with similar radiometric ages are well known from the broader region (e.g., Velence Mts., Transdanubian Range, UHER & ONDREJKA 2009; Tatra Mts., Hungarian Pannonian Basin, SZEMERÉDI et al. 2020; Western Carpathians, VILLASEÑOR et al. 2021).

3) Yet another alternative interpretation is that the dacite sample is in fact an extrusive rock providing a direct Permian stratigraphic age for the clastic sequence at 1930-1937 m depth in the Porrau-2 well.

The most probable age of the metadolerite sampled at 1816–1821 m depth is the age of the biotite rich sample (135.9±2.4 Ma). The other, older age imply that the K/Ar dating technique occasionally produces anomalously old ages attributed to excess argon in the case of altered rock samples. The excess argon in fluids being introduced into minerals or removed from minerals as grain boundary fluids during flow through a rock and is often concentrated in inclusions within minerals. The verification of this idea requires more detailed petrographic and analytical (geochemistry, geochronology) studies.

The radiometric ages measured on the dacite samples (ca. 283 Ma) are probably true geological ages and suggests that the lower part of the assumed Dogger sequence is actually Early Permian or Carboniferous in age. We indicated our new age assignments on Figure 3. This new age assignment for the lower part of the Porrau-2 well is consistent with the presence of the Permian and Upper Carboniferous clastics within the Boskovice Trough (NEHYBA et al. 2012), which extends from the Czech Republic southwards to our area as depicted by the regional transect (Figure 3).

Figure 10. a) Age (Ma) vs. K (%) plot of the samples and b) <sup>40</sup>Ar<sub>rad</sub> vs. K (%) plot of the samples10. ábra. a) A minták kora (Ma) vs. K (%) diagramja és b) a minták <sup>40</sup>Ar<sub>rad</sub> vs. K (%) diagramja

### Detrital zircon U-Pb and (U-Th)/He geochronology

A single coarse-grained sandstone sample was chosen for LA-ICP-MS detrital zircon U-Pb geochronology (Table V, see online digital supplement) from 1819 m depth (Figure 5). The relative probability distribution curve of U-Pb dates measured on 123 zircons display the characteristics of many other Dogger sandstones in the area (Figure 11, Table V), based on OMV's unpublished data sets.

Several prominent age populations were identified in the of the zircon data. These include, among others, “Variscan”, that is c. 330–350 Ma components, and an older, broader zircon population with ages between 540 and 640 Ma which is interpreted as “Cadomian” (Figure 11). The most dominant signal among the samples is the presence of a Variscan (Hercynian) peak with a 320–340 Ma age range interpreted to be derived from granitic plutons well known in the Bohemian Massif (KOŠLER et al. 2014). At least two recycling stages of the Variscan zircons are assumed: first to the Permian clastic sequence of the Boskovice Trough (Figure 3), and then to the Middle Jurassic sands. This recycling process could explain the relatively high quartz content of the Dogger sandstones (Table III). In particular, the sample analyzed shows the largest peak from Variscan zircons and could indicate the proximity of the to the Carboniferous Thaya pluton nearby (NEHYBA et al. 2012).

The second most prominent population is a Cadomian peak, clustering around 600 Ma (Ediacaran). The multi-stage recycling process of the zircons from the Cadomian and Caledonian units, like those of the Variscan ones, could have been a very prevalent process to provide such large proportion of zircons into the Dogger sequence.

The five youngest U-Pb dates are highlighted in Figure 11, which are dispersed between the Middle Triassic and the Upper Carboniferous (245–310 Ma). The single Middle Triassic zircon grain (245 Ma) is important as it excludes the Permian depositional age for this sandstone interval in the Porrau-2 well.

The five zircon (U-Th)/He dates (Table VI) from the same coarse-grained sandstone sample are between 214–303 Ma. The nominal closure temperature of the zircon (U-Th)/He system is ~180 °C, indicating that the zircon grains in this Middle Jurassic sandstone are likely recording Late Triassic cooling (below 200 °C) in the source region. Also, the data indicate that the sandstone sample probably never experienced temperature >180 °C since its deposition, which is consistent with detrital zircon fission track data from Late Cretaceous to Middle Miocene sediments from other wells drilled within the Vienna Basin (TAGAMI et al. 1996).

We indicated our new age assignments of the Porrau-2 well on Figure 5. The K-Ar dates on two biotite-rich fractions of the metadolerite in Sample #1 at 1816 m depth provided Hauterivian to Valanginian ages (135.9±2.4 Ma and 141.2±2.5 Ma). We consider these as true geologic age determinations as opposed to the one made on feldspar-rich separate from the same sample with a 231.78±4.04 Ma re-

sult. The latter age is interpreted to be affected by secondary processes. Similarly, the analytical ages obtained on Sample #2 with its apparent older age population and large dispersion between the three separates (243.8±4.8 Ma to 268.4±5.2 Ma; Middle Triassic–Middle Permian) must be the reflection of mixed dates. Alternatively, if these ages are geological then the sequence at the depth of 1855 m is not Dogger in age but at least as old as Permian to host a sill in it (Figure 5).

The very important dacite Sample #5 from 1937 m depth is interpreted as an older, Lower Permian sill (or lava unit?) based on the K-Ar dating (283.21±5.11 Ma and 284.37±4.97 Ma). However, this supposedly Dogger sequence of the Porrau-2 well (WIESENER 1965) cannot host a Permian age sill (Figure 5). Therefore, this part of the Porrau-2 well must be older than Lower Permian (Artinskian). In our view, some of the alluvial-fluvial clastics in the Porrau-2 and Roggendorf-1 wells represent the subsurface southwestern continuation of the Carboniferous–Permian Boskovice Trough from Moravia into Lower Austria (Figure 3). Also considering the detrital zircon geochronology (Figure 11), indirectly constraining the Dogger age at 1819 m depth, an important unconformity must exist between the Middle Jurassic and the Upper Paleozoic sequence in the Porrau-2 well (Figure 5). The location of this unconformity is somewhere between 1819–1937 m. Only with additional analysis and future data sets can the position of the unconformity be better constrained.

### Outlook for future work

Our preliminary results highlight the need for additional work, on both the volcanics and the sediments in both the Porrau-2 and Roggendorf-1 well. Considering that only one dacitic sample was dated, this age result should be considered as preliminary. The highly altered volcanics are obviously not ideal at all for K/Ar age dating, however, there are no alternatives for sampling unaltered rocks in these two wells. With additional K/Ar analyses on additional mineral fractions separated from representative dacitic core samples of drillhole Porrau-2 a more precise age control of the dacitic magmatism could be achieved. Also, in a dacitic rock, there is a chance to find zircons, which could give a much more robust age by U-Pb dating.

To establish a more specific comparison between the volcanics in Lower Austria and those known in the External Carpathians (Silesian Beskid Mts.) and the Western Carpathians of Poland and Slovakia, trace element geochemistry should be used. This approach should focus on highfield-strength elements (HFSE) since these are less affected by alteration. HFSE include all trivalent and tetravalent ions including the rare earth elements, the platinum group elements, uranium and thorium.

Additional petrographic analysis is required on the core materials of the Porrau-2 well with sandstone and conglomerate units (Figure 5). At some intervals, the metadolerites



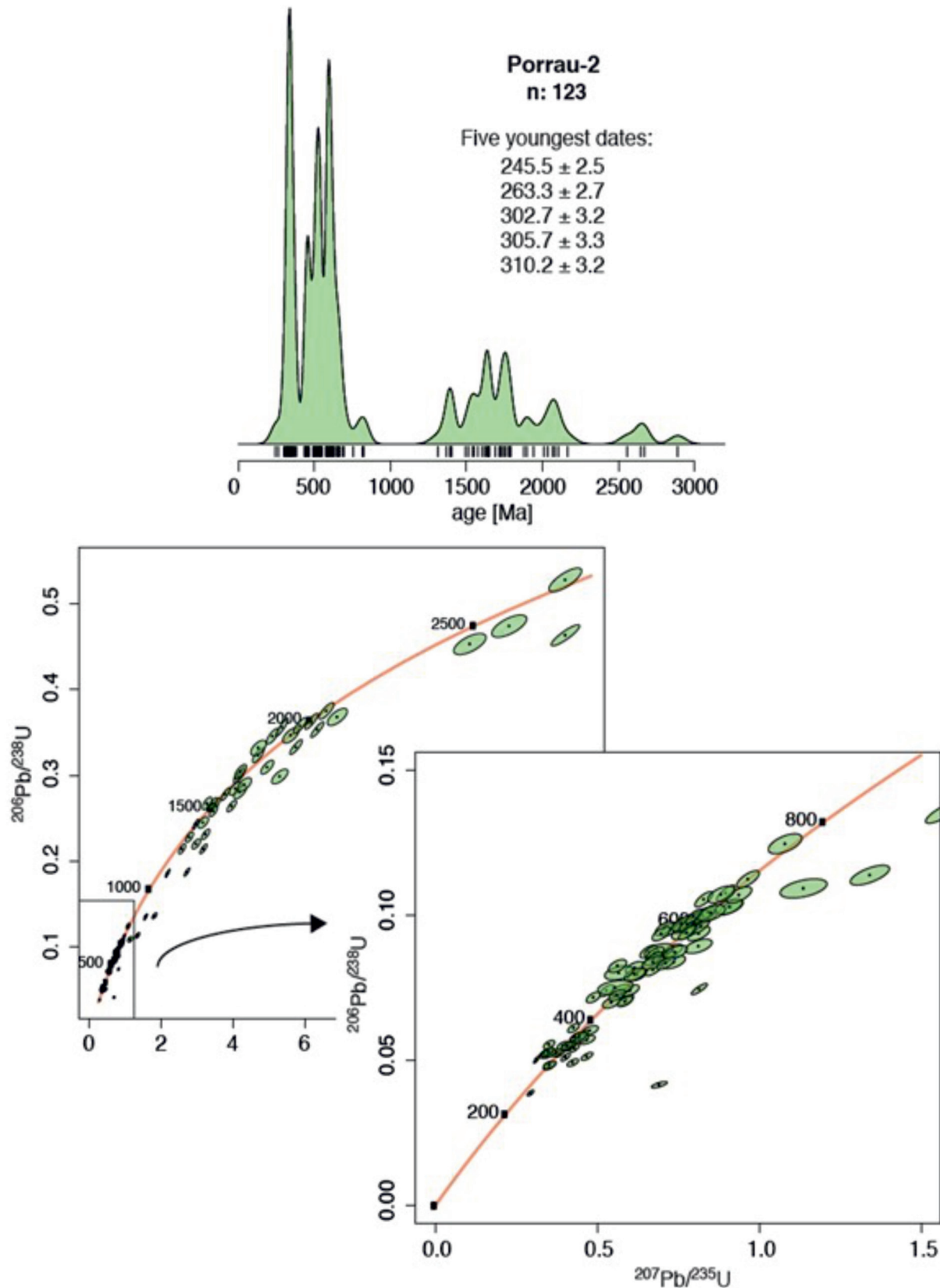


**Figure 11.** U-Pb Concordia diagram of detrital zircon analyses (n: 123) from sandstone Sample #1 at 1819 m. Note the presence of various populations, i.e. "Variscan" (330–350 Ma) age components and an older, broader zircon population with ages between 540 and 640 Ma which is interpreted as "Cadomian". The five youngest dates are 245–310 Ma

**11. ábra.** Cirkon U-Pb koradatok az 1819 m-ről származó #1 homokkőmintán 123 egyedi szemcse elemzésével. Vegyük észre a különböző populációk jelenlétét, azaz a „variszkuszi”, (330–350 Ma) korú és egy idősebb, szélesebb cirkonpopulációt 540 és 640 Ma közötti koradatokkal, amelyet „kadomiaai” korúnak értelmezzünk. Az öt legfiatalabb koradat az 245–310 Ma

**Table VI.** Uranium-Thorium/Helium age dating of 5 single grain zircons, Porrau-2 well, NE Austria. “Ft” is fraction of alphas retained, “corrected date” is corrected for this effect

*VI. táblázat.* Urán-tórium/hélium koreredmények 5 egyedi cirkonkristályon, Porrau-2 fúrás, ÉK-Ausztria. „Ft” a megtartott alfák töredéke, a „korrigált kor” erre a hatásra korrigált

| Full Sample Name | 4He (nmol/g) | ±     | U (ppm) | ±    | Th (ppm) | ±    | eU    | 4He (ncc) | ±     | Re (%) | U (ng) | ±     | Th (ng) | ±     | Th/U  | Raw Date It (Ma) | ±    | Ft    | Corrected Date (It) (Ma) | Analytic Unc. (Ma)2s |
|------------------|--------------|-------|---------|------|----------|------|-------|-----------|-------|--------|--------|-------|---------|-------|-------|------------------|------|-------|--------------------------|----------------------|
| POR2_01          | 722,966      | 2,404 | 635,88  | 8,42 | 113,55   | 2,38 | 662,6 | 51,215    | 0,170 | 100,0  | 2,0098 | 0,027 | 0,3589  | 0,008 | 0,179 | 198,88           | 2,54 | 0,737 | 268,14                   | 6,94                 |
| POR2_02          | 500,920      | 1,770 | 363,67  | 8,15 | 100,17   | 3,73 | 387,2 | 74,204    | 0,262 | 100,0  | 2,4036 | 0,054 | 0,6621  | 0,025 | 0,275 | 235,02           | 4,89 | 0,811 | 288,21                   | 12,04                |
| POR2_03          | 250,816      | 0,945 | 201,64  | 6,02 | 93,49    | 1,99 | 223,6 | 7,341     | 0,028 | 100,0  | 0,2633 | 0,008 | 0,1221  | 0,003 | 0,464 | 204,38           | 5,40 | 0,666 | 303,90                   | 16,14                |
| POR2_04          | 221,301      | 0,952 | 228,53  | 3,06 | 95,70    | 1,00 | 251,3 | 14,438    | 0,062 | 100,0  | 0,6652 | 0,009 | 0,2786  | 0,003 | 0,419 | 161,25           | 2,03 | 0,748 | 214,51                   | 5,41                 |
| POR2_05          | 659,972      | 2,280 | 651,37  | 7,91 | 122,05   | 1,33 | 680,4 | 101,202   | 0,350 | 100,0  | 4,4563 | 0,054 | 0,8350  | 0,009 | 0,187 | 177,24           | 2,09 | 0,793 | 222,67                   | 5,31                 |

are overlain by sandstones-conglomerates, which have volcanic components in them. If the basaltic material has been indeed reworked by the sandstones that would indicate the presence of at least some lavas in the sequence instead of only sills, which would hold to constrain the age relationships.

Similarly, the tuffs and tuffites reported from both the Porrau-2 and Roggendorf-1 wells suggest the presence of extrusive volcanism. We are not aware of Middle Jurassic volcanism anywhere close to our study area; however, Permian volcanism is known in the broader region (NEHYBA et al. 2012).

As to the future detailed analysis of the sandstones, their petrographic composition should be different for the Middle Jurassic versus Permian or Carboniferous units. Additional detrital zircon analysis beyond the singular sample (*Figure 11*) used in this study could be used as a discriminating tool. Also, the multiple coal and coaly shale intervals described in the Porrau-2 well should be analyzed as their characteristics might be different for Middle Jurassic versus Carboniferous coals described in the broader region.

Finally, our efforts focused solely on the Porrau-2 well, but the volcanic materials in the Roggendorf-1 well cores should be also revisited after the pioneering early study by WIESENER (1965). The intense alteration of the volcanics observed in the Porrau-2 well which complicated the use of the K-Ar age dating, may not be present in the Roggendorf-1 well.

### Regional implications

The recognition of Lower Cretaceous sills in NE Austria has some large-scale paleogeographic and geodynamic implications. It is not only the age, but also the overall petrographic nature of the Porrau-2 sills that is similar to the well-known Lower Cretaceous alkaline igneous rocks (lamprophyres, basanites, phonolites) occurring in the Moravian-Silesian Beskidy area in NE Czech Republic, southern Poland and in the Mecsek Zone of southern Hungary.

The Early Cretaceous continental mafic alkaline rift-type volcanic activity and extension ultimately led to the opening of Penninic oceanic rift arms (HARANGI et al. 1996). During the post-breakup extension phases did the slow-spreading oceanic ridges develop, which are characterized

by the MORB-type basaltic volcanism. Alkaline volcanic provinces have a linear character and were envisioned to follow the passive continental margins of the Penninic oceanic basins (HARANGI et al. 1996, SPIŠIAK et al. 2011).

Continental rift-type alkali basalt volcanism in the Hungarian part of the Tisza Mega-unit reached its paroxysm during the Early Cretaceous. The volcanic centers were located in the Mecsek Mts. and the Szolnok Unit based on subsurface data sets (SZEPEŠHÁZY 1977, MOLNÁR 1985, BÉRCZIMÁK 1986, HAAS et al. 2010), but its traces were also encountered in the Villány–Bihor Unit (HAAS & PÉRO 2004). The main period of volcanism at about 130 Ma roughly coincides with a major change reflected in the palaeomagnetic declinations in the Mecsek Mts. (MÁRTON 2000) marking the CCW rotation of the Tisza Mega-unit relative to stable Europe.

TARI (2018) suggested that in a paleogeographic sense Tisza had to be located to the west or southwest of the Bohemian Spur prior to its separation from the European margin during the Early Cretaceous (*Figure 12*). While there is an ongoing debate on the paleo-position of Tisza in relation to stable Europe, the studied two wells in Lower Austria provide a fixed position for at least a segment of the Early Cretaceous rift system involving several mega-units in the broader Alpine–Carpathian–Pannonian realm (cf. SPIŠIAK et al. 2011).

### Conclusions

The occurrences of numerous sills penetrated in two deep exploration wells drilled in the Molasse Basin in northeast Austria were known since the early 1960s. Although the initial analysis of these metadolerite units intercepted in a supposedly Dogger (Porrau-2) and Upper Paleozoic (Roggendorf-1) clastic sequence correctly concluded their intrusive character, the age relationships and the broader stratigraphic and tectonic implications remained poorly constrained.

After about 60 years, using various modern analytical methods, a new understanding of these intrusives is outlined in this contribution. Originally, the age of the various metadolerites was considered as Jurassic. However, our new results provided an Early Cretaceous age (136–141 Ma) for the intrusive volcanism not only indicated by K-Ar age determination and but also by regional analogues for the sills.



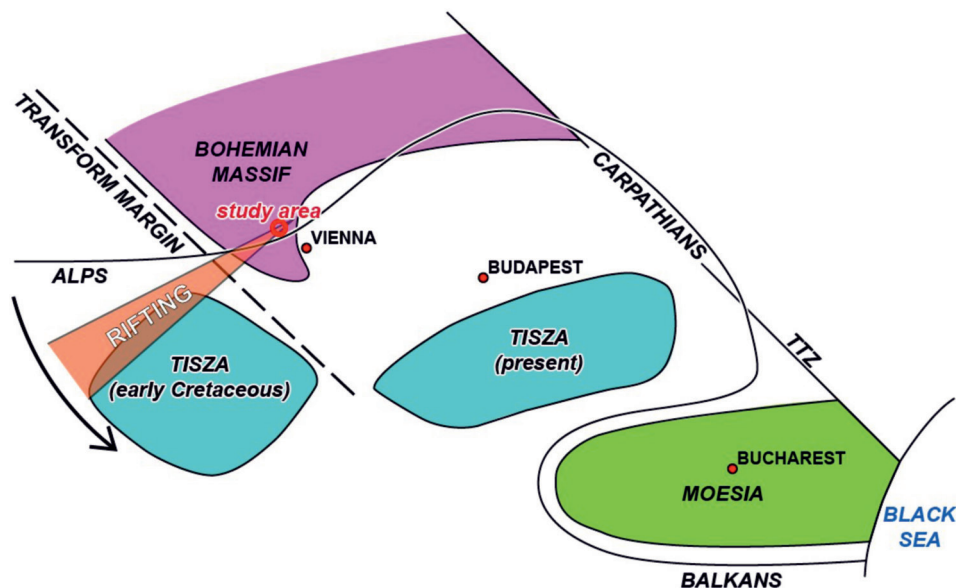


**Figure 12.** Cartoon model of the Early Cretaceous rifting along the southern edge of the European margin with implications for the Tisza Mega-unit (modified from TARI 2018). Not drawn to scale, TTZ, Teisseyre-Tornquist Zone. Other intra-Carpathian units, such as ALCAPA and Dacia, are omitted for clarity. The documented CCW rotation of Tisza during the Early Cretaceous (MÁRTON 2000) coincided with the continental rifting along its northern perimeter. The along-strike, northeastern continuation of the rift zone is interpreted to extend to our study area on the autochthonous eastern flank of the Bohemian Massif (Figure 1).

**12. ábra.** Az európai perem déli peremén végbement kora kréta kori riftesedés rajzos modellje a Tisza mega-egységre vonatkozó következményekkel (TARI 2018 alapján módosítva). Nem méretarányosan rajzolta, TTZ, Teisseyre-Tornquist zóna. Más Kárpátokon belüli egységek, mint az ALCAPA és a Dácia, az áttekinthetőség kedvéért kihagyva. A Tisza mega-egység óramutató járásával ellentétes irányú forgása a korai kréta idején (MÁRTON 2000) egybeesett az északi peremén végbement kontinentális riftesedéssel. A riftmedence csapásmenti, ÉK-i folytatását úgy értelmezzük, hogy az a mi vizsgálati területünkre is kiterjed a bohemiai masszívum autochton keleti szárnyán (1. ábra).

A single dacite sill from the lower, supposedly Dogger sequence of the Porrau-2 well is interpreted as an older intrusive unit and its K-Ar dating (283–284 Ma) suggests a Early Permian age. Hence the sequence penetrated in the deeper part of this well cannot be Dogger in age but instead, it is Upper Paleozoic (Permian). Therefore, some of the alluvial-fluvial clastics in the Porrau-2 and Roggendorf-1 wells represent the southwestern continuation of the Carboniferous–Permian Boskoviце Trough from Moravia into Lower Austria (Figure 3).

## Acknowledgements

We are pleased to thank Prof. Csaba SZABÓ for everything we learned from him regarding petrology during our university years and beyond. Part of this work was done in the framework of an OMV Upstream Technology Project (No. F.1019016) in 2019–2020. Comments by Réka LUKÁCS, Sanja ŠUICA and Ján SPIŠIAK were used to produce a final version of this paper.

## References – Irodalom

- ANDERSEN, T. 2002: Correction of common lead in U-Pb analyses that do not report  $^{204}\text{Pb}$ . – *Chemical Geology* **192**, 59–79. [https://doi.org/10.1016/s0009-2541\(02\)00195-x](https://doi.org/10.1016/s0009-2541(02)00195-x)
- BÉRCZI-MAKK, A. 1986: Mesozoic formation types of the Great Hungarian Plain. – *Acta Geologica Hungarica* **29**, 261–282.
- BRIX, F. 1993: Molasse und deren Untergrund östlich und südöstlich der Böhmisches Masse – östliches Niederösterreich. – In: BRIX, F. & SCHULTZ, O. (Eds.): *Erdöl und Erdgas in Österreich*, 2. edition, 323–358, Wien.
- BRIX, F. & GÖTZINGER, K. 1964: Die Ergebnisse der Aufschlußarbeiten der OMV AG in der Molassezone Niederösterreichs in den Jahren 1957–1963. Teil I. Zur Geologie der Beckenfüllung, des Rahmens und des Untergrundes. – *Erdöl-Zeitung* **80**, 57–76.
- CASSIGNOL, C. & GILLOT, P.-Y. 1982: Range and effectiveness of unspiked potassium-argon dating: experimental groundwork and applications. – In: *Numerical Dating in Stratigraphy*, John Wiley & Sons, 159–179.
- CSIBRI, T., PLAŠIENKA, D. & DEMKO, R. 2020: Occurrence of Lower Cretaceous magmatic rocks between Podbranč village and Myjava town. – *Geologické Práce Správy* **136**, 33–38.
- DALRYMPLE, G. B. & LANPHERE, M. A. 1969: *Potassium-argon dating. Principles, techniques and applications to geochronology*. – U.S. Geological Survey, Freeman and Company, San Francisco, p. 257.

On a regional scale, the petrography of the studied sills is similar to the characteristics of the well-studied Lower Cretaceous alkaline igneous rocks (lamprophyres, basanites, phonolites) occurring in the Moravian-Silesian Beskidy area in northeastern Czech Republic and southern Poland and also in the Mecsek Zone of southern Hungary. Although all these volcanic units are presently located in Alpine thrust-fold belts displaced from their original paleogeographic position, the metadolerite sills in our study are anchored within the autochthonous European plate. Therefore, they provide an important new constraint for the palinspastic reconstruction of the regional-scale Early Cretaceous rift zone along the southern margin of the Mesozoic European plate.

- GILLOT, P. & CORNETTE, Y. 1986: The Cassinol technique for potassium-argon dating. precision and accuracy: Examples from the late pleistocene to recent volcanics from Southern Italy. – *Chemical Geology: Isotope Geoscience section* **59**, 205–222. [https://doi.org/10.1016/0168-9622\(86\)90099-0](https://doi.org/10.1016/0168-9622(86)90099-0)
- HAAS, J. & PÉRO, C. 2004: Mesozoic evolution of the Tisza Mega-unit. – *International Journal of Earth Sciences* **93**, 297–313. <https://doi.org/10.1007/s00531-004-0384-9>
- HARANGI, SZ. 1994: Geochemistry and petrogenesis of the Early Cretaceous continental rift-type volcanic rocks of the Mecsek Mountains, south Hungary. – *Lithos* **33**, 303–321. [https://doi.org/10.1016/0024-4937\(94\)90035-3](https://doi.org/10.1016/0024-4937(94)90035-3)
- HARANGI, SZ. & ÁRVA-SÓS, E. 1993: The Early Cretaceous volcanic rocks in the Mecsek Mts. (South Hungary). – *Földtani Közöny* **123**, 129–165.
- HARANGI, SZ., SZABÓ, CS., JÓZSA, S., SZOLDÁN, Z., ÁRVA-SÓS, E., BALLA, M. & KUBOVICS, I., 1996: Mesozoic igneous suites in Hungary: Implications for genesis and tectonic setting in the northwestern part of Tethys. – *International Geology Review* **38**, 336–360. <https://doi.org/10.1080/00206819709465339>
- HARANGI, SZ., TONARINI, S., VASELLI, O. & MANETTI, P. 2003: Geochemistry and petrogenesis of Early Cretaceous alkaline igneous rocks in Central Europe: Implications for a long-lived EAR-type mantle component beneath Europe. – *Acta Geologica Hungarica* **46**, 77–94. <https://doi.org/10.1556/ageol.46.2003.1.6>
- HESS J. C. & LIPPOLT H. J. 1994: Compilation of K-Ar measurements on HDB-1 standard biotite 1994 status report. in: Odin G.S. (ed): Phanerozoic Time Scale. – *Bulletin of Liaison and Information of the IUGS Subcommittee* **12**, 19–21.
- HNYLKO, O., KROBICKI, M., FELDMAN-OLSZEWSKA, A. & IWAŃCZUK, J. 2015: Geology of the volcano-sedimentary complex of the Kamyanyi Potik Unit on Chyvchyn Mount (Ukrainian Carpathians): preliminary results. – *Geological Quarterly* **59**, 145–156. <https://doi.org/10.7306/gq.1220>
- IRVINE, T. N., & BARAGAR, W. 1971: A guide to the chemical classification of the common volcanic rocks. – *Canadian Journal of Earth Sciences* **8**, 523–548. <https://doi.org/10.1139/e71-055>
- KOŠLER, J., KONOPÁSEK, J., SLÁMA, J. & VRÁNA, S. 2014: U–Pb zircon provenance of Moldanubian metasediments in the Bohemian Massif. – *Journal of the Geological Society* **171**, 83–95. <https://doi.org/10.1144/jgs2013-059>
- KROBICKI, M., FELDMAN-OLSZEWSKA, A., HNYLKO, O. & IWAŃCZUK, J. 2019: Peperites and other volcano-sedimentary deposits (lowermost Cretaceous, Berriasian) of the Ukrainian Carpathians. – *Geologica Carpathica* **70**, 146–150.
- KRÖLL, A. & WESSELY, G. 2001: Geologische Karte der Molassebasis 1: 200000. – In: *Geologische Themenkarten der Republik Österreich: Molassezone Niederösterreich und angrenzende Gebiete 1:200000*, Wien, Geologische Bundesanstalt.
- KUBOVICS, I. & BILLIK, I. 1984: Comparative investigations of the Hungarian Mesozoic mafic–ultramafic and some ophiolitic magmatic rocks in the Alp–Carpathian chain. – *Acta Geologica Hungarica* **27**, 321–339.
- KUBOVICS, I., SZABÓ, CS., HARANGI, SZ. & JÓZSA, S. 1990: Petrology, petrochemistry of Mesozoic magmatic suites in Hungary, adjacent areas – an overview. – *Acta Geodaetica et Geophysica Hungarica* **25**, 345–371.
- KUNO, H. 1968: Differentiation of basalt magmas. – In: HESS, H. H. & POLDERVAART, A. (Eds.) *Basalts: The Poldervaart treatise on rocks of basaltic composition*. Interscience Publishers, New York, 623–688.
- LE BAS, M. J., LE MAITRE, R. W., STRECKEISEN, A., ZANETTIN, B. & IUGS Subcommittee on the Systematics of Igneous Rocks 1986: A Chemical Classification of Volcanic Rocks Based on the Total Alkali-Silica Diagram. – *Journal of Petrology* **27/3**, 745–750. <https://doi.org/10.1093/petrology/27.3.745>
- MADZIN, J., SÝKORA, M. & SOTÁK, J. 2014: Stratigraphic position of alkaline volcanic rocks in the autochthonous cover of the High-Tatric Unit (Western Tatra Mts., Central Western Carpathians, Slovakia). – *Geological Quarterly* **58**, 163–180. <https://doi.org/10.7306/gq.1147>
- MÁRTON, E. 2000: The Tisza Megatectonic Unit in the light of paleomagnetic data. – *Acta Geologica Hungarica* **43**, 329–343.
- McFARLANE, C. R. M. & LUO, Y. 2012: U-Pb geochronology using 193 nm Excimer LA-ICP-MS optimized for in situ accessory mineral dating in thin sections. – *Geoscience Canada* **39**, 158–172.
- MOLNÁR, S. 1985: Petrochemical character of the Lower Cretaceous volcanic rocks of the Great Hungarian Plain. – *Acta Mineralógica–Petrographica* **27**, 33–38.
- NEHYBA, S., ROETZEL, R. & MAŠTERA, L. 2012: Provenance analysis of the Permo-Carboniferous fluvial sandstones of the southern part of the Boskovice Basin and the Zöbing Area (Czech Republic, Austria): implications for paleogeographical reconstructions of the post-Variscan collapse basins. – *Geologica Carpathica* **63**, 365–382. <https://doi.org/10.2478/v10096-012-0029-z>
- ODIN, G. S. 1982: *Numerical Dating in Stratigraphy*. – John Wiley & Sons, Chichester–New York–Brisbane–Toronto–Singapore.
- QUIDELLEUR, X., GILLOT, P. Y., SOLER, V. & LEFÈVRE, J. C. 2001: K/Ar dating extended into the last millennium: Application to the youngest effusive episode of the Teide volcano (Spain). – *Geophysical Research Letters* **28**, 3067–3070. <https://doi.org/10.1029/2000GL012821>
- ROETZEL, R., AHL, A., GÖTZINGER, M. A., KOCIU, A., PRISTACZ, H., SCHUBERT, G., SLAPINSKY, P. & WESSELY, G. 2009: Erläuterungen zu Blatt 23 Hadres. – *Geologische Karte der Republik Österreich* **1**, 151 p.
- ROLLINSON, H. & PEASE, V. 2021: *Using Geochemical Data to Understand Geological Processes*. – Second Edition, Cambridge University Press, Cambridge.
- SCHWARZ, W.H. & TRIELOFF, M. 2007: Intercalibration of <sup>40</sup>Ar–<sup>39</sup>Ar age standards NL-25, HB3gr hornblende, GA1550, SB-3, HD-B1 biotite and BMus/2 muscovite. – *Chemical Geology* **242**, 218–231. <https://doi.org/10.1016/j.chemgeo.2007.03.016>
- SLÁMA, J., KOSLER, J., CONDON, D. J., CROWLEY, J. L., GERDES, A., HANCHAR, J. M., HORSTWOOD, M., MORRIS, G. A., NASDALA, L., NORBERG, N., SCHALTEGGER, U., SCHOENE, B., TUBRETT, M. N. & WHITEHOUSE, M. J. 2008: Plesovice zircon – a new natural reference material for U–Pb and Hf isotopic microanalysis. – *Chemical Geology* **249**, 1–35. <https://doi.org/10.1016/j.chemgeo.2007.11.005>



- SPIŠIAK, J. 2002: Mesozoic alkali basalts/lamprophyres from the Western Carpathians. – *Geologica Carpathica* **53**, 183–185.
- SPIŠIAK, J., PLAŠIENKA, D., BUČOVÁ J., MIKUŠ T. & UHER P. 2011: Petrology and palaeotectonic setting of Cretaceous alkaline basaltic volcanism in the Pieniny Klippen Belt (Western Carpathians, Slovakia). – *Geological Quarterly* **55**, 27–48.
- SPRÁNITZ, T., TARI, G., PORKOLÁB, K., VRŠIC, A., HUJER, W., MEKONNEN, E. & BERKESI, M. 2024: Geoenergy re-evaluation of the Szombathely-II well, western Hungary: a tribute to Prof. Csaba SZABÓ. – *Földtani Közlöny* **154/3**, 277–298. <https://doi.org/10.23928/foldt.kozl.2024.154.3.277>
- STEIGER, R. H. & JÁGER, E. J. 1977: Subcommission on geochronology: Convention on the use of decay constants in geo- and cosmochronology. – *Earth and Planetary Science Letters* **36**, 359–362. [https://doi.org/10.1016/0012-821X\(77\)90060-7](https://doi.org/10.1016/0012-821X(77)90060-7)
- SZEMERÉDI, M., LUKÁCS, R., VARGA, A., DUNKL, I., JÓZSA, S., TATU, M., PÁL-MOLNÁR, E., SZEPESI, J., GUILLONG, M., SZAKMÁNY, Gy. & HARANGI, SZ. 2020: Permian felsic volcanic rocks in the Pannonian Basin (Hungary): new petrographic, geochemical, and geochronological results. – *International Journal of Earth Sciences* **109**, 101–125. <https://doi.org/10.1007/s00531-019-01791-x>
- SZEPESHÁZY, K. 1977: Mesozoic igneous rocks of the Great Hungarian Plain. – *Földtani Közlöny* **107**, 384–397.
- SZOPA, K., WŁODYKA, R. & CHEW, D. 2014: LA-ICP-MS U-Pb apatite dating of Lower Cretaceous rocks from teschenite-picrite association in the Silesian Unit (Southern Poland). – *Geologica Carpathica* **65**, 273–284. <https://doi.org/10.2478/geoca-2014-0018>
- TAGAMI, T., CARTER, A. & HURFORD, A. J. 1996: Natural long-term annealing of the zircon fission-track system in Vienna Basin deep borehole samples: constraints upon the partial annealing zone and closure temperature. – *Chemical Geology* **130**, 147–157. [https://doi.org/10.1016/0009-2541\(96\)00016-2](https://doi.org/10.1016/0009-2541(96)00016-2)
- TARI, G. 2005: The divergent continental margins of the Jurassic proto-Pannonian Basin: implications for the petroleum systems of the Vienna Basin and the Moesian Platform. – *Transactions GCSSEPM Foundation Annual Research Conference, Houston, Texas* **25**, 955–986.
- TARI, G. 2018: Where was the Tisza micro-plate located on the European margin? – In: ŠUJAN, M., CSIBRI, T., KISS, P. & RYBÁR, S. (Eds.): *Environmental, Structural and Stratigraphical Evolution of the Western Carpathians: 11th ESSEWECA Conference, Abstract Book*, November 29–30, 2018, Bratislava, Slovakia, 121–124.
- UHER, P. & ONDREJKA, M. 2009: The Velence granites, Transdanubic Superunit: a product of Permian A-type magmatism and Alpine overprint (results of zircon SHRIMP and monazite EMPA dating). – *HUNTEK 2009, Proceedings of the 7th Meeting of the Central European Tectonic Studies Group (CETeG) and 14th Meeting of the Czech Tectonic Studies Group (CTS) Pécs, Hungary Volume: HUNTEK-2009, Abstracts*, p. 32.
- VERMEESCH, P. 2018: IsoplotR: a free and open toolbox for geochronology. – *Geoscience Frontiers* **9**, 1479–1493. <https://doi.org/10.1016/j.gsf.2018.04.001>
- VERMEESCH, P. & PEASE, V. 2021: A genetic classification of the tholeiitic and calc-alkaline magma series. – *Geochemical Perspectives Letters* **19**, 1–6. <https://doi.org/10.7185/geochemlet.2125>
- WESSELY, G. 2006: Sedimente des Paläozoikums und Mesozoikums unter der Molasse. – In: WESSELY, G. (Ed.): *Geologie der Österreichischen Bundesländer: Niederösterreich*, 59–66, Wien, Geologische Bundesanstalt.
- WIEDENBECK, M., ALLEN, P., CORFU, F., GRIFFIN, W. L., MEIER, M., OBERLI, F., VON QUADT, A., RODDICK, J. C. & SPIEGEL, W. 1995: Three natural zircon standards for U-Th-Pb, Lu-Hf, trace element and REE analyses. – *Geostandards and Geoanalytical Research* **19**, 1–23. <https://doi.org/10.1111/j.1751-908X.1995.tb00147.x>
- VILLASEÑOR, G., CATLOS, E. J., BROSKA, I., KOHÚT, M., HRAŠKOD, L., AGUILERA, K., KYLE, R. J. & STOCKLI, D. F. 2021: Evidence for widespread mid-Permian magmatic activity related to rifting following the Variscan orogeny (Western Carpathians). – *Lithos* **390–391**. <https://doi.org/10.1016/j.lithos.2021.106083>
- WIESENER, H. 1965: Vulkanite im Untergrund der Molassezone Niederösterreichs: Ein Beitrag zur Spilitfrage. – *Tschermaks mineralogische und petrographische Mitteilungen* **10**, 157–169. <https://doi.org/10.1007/bf01128624>
- WIESENER, H., FREILINGER, G., KITTLER, G. & TSAMBOURAKIS, G. 1976: Der kristalline Untergrund der Nordalpen in Österreich. – *Geologische Rundschau* **65**, 512–525. <https://doi.org/10.1007/bf01808478>

Manuscript received: 19/03/2024

### Digital supplementary

Table V. LA-ICP-MS U-Pb zircon analysis, Porrau-2 well, NE Austria

V. táblázat. Lézerablációs induktívan kapcsolt plazma tömegspektrometriás uránium-ólom kor eredmények cirkon kristályokon, Porrau-2 fúrás, ÉK-Ausztria